TECHNICAL REPORT

ISO/TR 15657

First edition
2013-06-15

Fire resistance tests — Guidelines for computational structural fire design

Essais de résistance au feu — Lignes directrices sur la conception statistique des feux de structures

COPYRIGHT PROTECTED DOCUMENT

Contents

Page

Foreword

ISO (the International Organization for Standardization) is a worldwide federation of national standards bodies (ISO member bodies). The work of preparing International Standards is normally carried out through ISO technical committees. Each member body interested in a subject for which a technical committee has been established has the right to be represented on that committee. International organizations, governmental and non-governmental, in liaison with ISO, also take part in the work. ISO collaborates closely with the International Electrotechnical Commission (IEC) on all matters of electrotechnical standardization.

The procedures used to develop this document and those intended for its further maintenance are described in the ISO/IEC Directives, Part 1. In particular the different approval criteria needed for the different types of ISO documents should be noted. This document was drafted in accordance with the editorial rules of the ISO/IEC Directives, Part 2. www.iso.org/directives

Attention is drawn to the possibility that some of the elements of this document may be the subject of patent rights. ISO shall not be held responsible for identifying any or all such patent rights. Details of any patent rights identified during the development of the document will be in the Introduction and/or on the ISO list of patent declarations received. www.iso.org/patents

Any trade name used in this document is information given for the convenience of users and does not constitute an endorsement.

The committee responsible for this document is ISO/TC 92, *Fire safety*, Subcommittee SC 2, *Fire containment*.

Introduction

In recent years significant advances have been made in the scientific community in understanding the behaviour of fire in building structures and as a result there is an increasing activity in the development of computer models that are capable of describing and predicting many of the different aspects of fire safety engineering.

As a result of this research, design codes have been prepared that enable practising engineers to undertake this type of analysis which can be applied to comply with prescriptive requirements as specified in National Building Regulations, or, to develop performance based fire safety strategies and often involving complex computational analysis.

In particular, analytical procedures and computer models have been developed in the areas of:

— reaction of materials to fire;

— fire growth in a compartment;

— fully developed compartment fire;

— fire spread between buildings;

— fire behaviour of load-bearing and separating elements and building structures;

— smoke filling in enclosures and smoke movement in escape routes and multi-story buildings;

— interaction of sprinklers and fire, including sprinkler and fire venting interaction;

— process of escape; and

— systems approach to the overall fire safety of a building, in its most general form comprising fire development models interacting with human response models.

This progress in fire research has led to consequent changes in the field of codes, specifications, and recommendations for fire engineering. Some characteristic trends in these changes are:

— improved relationship between standard tests and real fire scenarios;

— increased use of fire safety engineering principles to meet functional requirements and performance based criteria;

— development of new test methods, that are, as far as possible, material-independent and related to well-defined phenomena and properties;

— increase in the application of reliability-based analytical design;

— extended use of integrated assessments; and

— introduction of goal-oriented systems of analysis of total, active and passive fire protection for a building.

One of the most rapidly developing trends relates to the structural fire engineering design of load-bearing and separating structures. An analytical determination of the fire resistance of structural elements is being accepted more widely by the Approving Authorities in many countries as an alternative to the internationally prescriptive based approaches based on the results of the standard fire resistance test and connected classification.

A significant contribution to the analysis of building structures in fire has been made by the development of the European Structural Eurocodes which enable practising engineers to follow agreed design procedures for application in individual members states. During the mid 1990s, these Codes which covered; Fire Actions and individual structural materials (Concrete, Steel, Composite Steel and Concrete, Timber, Masonry, Aluminium) were published as ENV's (or pre-standards). These Codes had the status of Draft for Development, and were supplemented with National Applications Documents (NAD's), which

permitted member states to ascribe certain factors to many of the calculations and input variables in order to align with National experience.

During the last five years, considerable progress has been made in converting these pre-standards into full European Design Codes for application in the European Community member states. The Codes are now divided into two separate parts:

— **Normative** - in which members states are obliged to follow.

— **Informative** - usually consisting of a series of Annexes in which acceptance is voluntary by individual member states.

In addition, there is still provision to apply individual National Determined Parameters (NDP's) to align more closely with National experience. The interaction of the Eurocodes are summarized in Figure 1.

```
┌─────────────────────────────────────────────┐
│  Selection of the relevant design fire scenarios │
│         Eurocode 1: Fire Actions             │
└─────────────────────────────────────────────┘
                      │
                      ▼
┌─────────────────────────────────────────────┐
│  Determination of the corresponding design fire │
│         Eurocode 1: Fire Actions             │
└─────────────────────────────────────────────┘
                      │
                      ▼
┌─────────────────────────────────────────────┐
│ Calculation of the temperature rise of the structural member │
│         Eurocodes 2-6 & 9: Fire Actions      │
└─────────────────────────────────────────────┘
                      │
                      ▼
┌─────────────────────────────────────────────┐
│     Calculation of the mechanical response   │
│         Eurocodes 2-6 & 9: Fire Actions      │
└─────────────────────────────────────────────┘
```
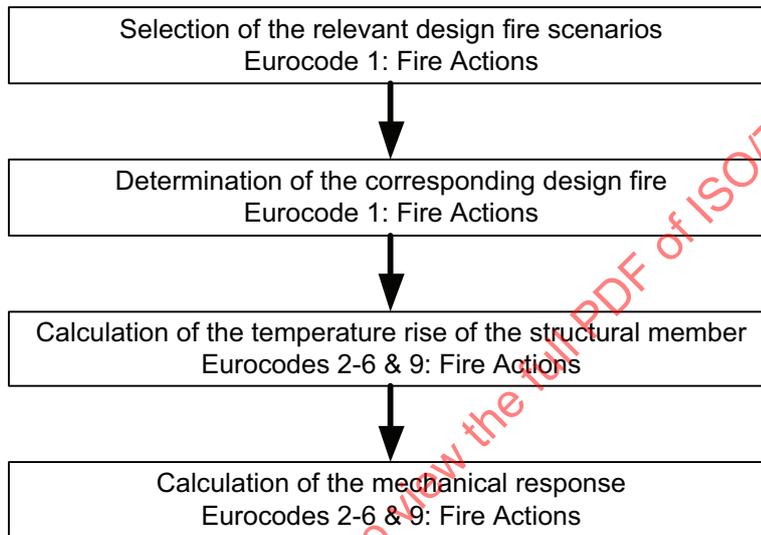
Figure 1 — Interaction of the Structural Eurocodes

The structural Fire Engineering design models have been reviewed in Reference [1] and essentially they can be presented in a simple form as three succinct design steps shown in Figure 2:

```
┌─────────────────────────┐
│     Fire Analysis        │
└─────────────────────────┘
             │
             ▼
┌─────────────────────────┐
│  Heat Transfer Analysis  │
└─────────────────────────┘
             │
             ▼
┌─────────────────────────┐
│   Structural Analysis    │
└─────────────────────────┘
```
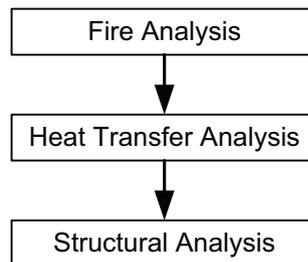
Figure 2 — Three stages to structural fire design

This report examines each of the above under separate headings. In each case, internationally applied methods for a structural fire engineering design are discussed.

For fire models or thermal actions the report considers:

Furnace tests:

— according to ISO 834: cellulosic, hydrocarbon, external and smouldering curves.

— tunnel heating curves according to RWS and the French National curve.

Natural fires:

— single zone or parametric fires in so far as they may be used in a standardised way to provide characteristic occupancy related standard tests. This also includes time equivalent relationships for quantifying real fires into an equivalent period of heating in the standard ISO 834 test.

For heat transfer models the report considers:

— Heat transfer for uniform temperature distribution

— Non-uniform temperature distribution for

  — one dimension

  — two dimensions

  — three dimensions

For structural models the report considers:

— Single member analysis

  — Sub-frame assembly analysis (sub-frames and assembly of members)

  — Global structural analysis in which load redistribution occurs.

The report also considers **Combination Models** for thermal and structural analysis and the performance of structural glass, plastics and resins.

In addressing structural models relevant thermo-physical and mechanical properties are presented for each loadbearing material. While these are presented for use in calculating the thermal response under standard furnace heating conditions for the most part the same properties will invariably be appropriate for natural fires.

This Technical Report is one of a series of Technical Reports being developed that provide guidance on important aspects of calculation methods for fire resistance of structures. Related documents include

— ISO/TR 15655, *Fire resistance — Tests for thermo-physical and mechanical properties of structural materials at elevated temperatures for fire engineering design*,

— ISO/TR 15656, *Fire resistance — Guidelines for evaluating the predictive capability of calculation models for structural fire behaviour*, and

— ISO/TR 15658, *Fire resistance tests — Guidelines for the design and conduct of non-furnace-based large-scale tests and simulation*.

Other documents, which have been produced in ISO/TC92/SC2, provide data and information on the determination of fire resistance. In particular, these include

— ISO 834 (all parts), *Fire resistance tests — Elements of Building Construction*,

— ISO/TR 12470, *Fire resistance tests — Guidance on the application and extension of results*,

— ISO/TR 12471, *Computational structural fire design — Review of calculation models, fire tests for determining input material data and needs for further development*, and

— ISO/TR 10158:1991[1)], *Principles and rationale underlying calculation methods in relation to fire resistance of structural elements*.

---

1) Withdrawn.

Fire resistance tests — Guidelines for computational structural fire design

1 Scope

This Technical Report provides an overview of the advances that have been made in understanding how structures respond to fire. This is reviewed in terms of heat transfer to the structural elements from primarily nominal (furnace) fires changes in the elevated temperature, physical and mechanical characteristics of structural materials, and how the information is used in the analysis of structural elements for the fire limit state. In reviewing the fire scenarios the report concentrates primarily on standardized heating curves but includes the basis of characteristic curves, which may at some time in the future be adopted in a standardized way. Reference is made to time equivalent as a recognized methodology in relating a natural or characteristic fire, to an equivalent period of heating in the ISO 834 furnace test.

This Technical Report is the result of the development of European Structural Eurocodes for application by member states in the European Community. These Codes enable practising engineers to follow agreed design procedures for application in individual members states irrespective of whether these are for building projects either inside or outside their own National boundaries.

The current UK national structural codes and the European (Eurocodes) are listed in Annex A.

2 Basic principles

2.1 Primary objectives of fire safety design

The primary objectives for fire safety design are

— Life safety - Regulatory requirements for the occupants, fire fighters and rescue services

— Property protection - Regulatory, societal, economic and insurance requirements

— Environmental protection - Regulatory, societal and insurance requirements

— Heritage - Regulatory and societal requirements

In order to limit the impact of fire risk accepted levels are reflected in national fire safety codes, which are generally expressed in terms of requirements and recommended measures. These set out to control the risk of ignition, fire growth and flashover, as well as their consequences and encompass the following strategies:

a) reducing the risk of occurrence,

b) control of fire (heat, flames, smoke and toxic gases) at an early stage,

c) ensuring a safe evacuation of people (and possibly of property), or safe areas of refuge,

d) preventing fire spread (heat, flames, smoke and toxic gases) beyond a certain area (compartmentation),

e) providing for safe and efficient operating conditions for the fire brigades and rescue services,

f) avoiding premature structural failure or limiting structural damage with respect to reinstatement,

g) minimising business interruption and financial losses,

h) minimising the impact upon the environment.

Structural fire safety design is directly concerned with strategies involving items (c) to (h) since these will come into play if the fire is not controlled at an early stage in its development.

The level of structural fire safety provided should be considered in terms of:

— the risk of fire occurring, which is considered as an accidental situation,

— the development of fire through:

  — compartment geometry

  — ventilation

  — fire loading

— the reduction in risk by introducing structural measures,

  — engineering design

  — materials selection

  — passive protection

— the reduction in risk by introducing fire compartments or containments that prevent fire spread beyond the surrounded area for a specific time. For some buildings, a complete floor may be regarded as a single compartment.

— the reduction in risk by the introduction of active protection measures (detection, alarm, sprinklers, smoke control, fire brigade).

2.2   Performance criteria

The level of structural fire safety can be evaluated by performance criteria depending of the strategy chosen.

For load-bearing structures, these are:

— load-bearing function for the whole duration of fire or a part of it (ultimate limit state),

— limit on the extent of deformation (deflection, displacement, contraction, elongation) with respect to the integrity of separating elements, or, for the fire protection material to remain attached to the load-bearing structure (deformation limit state),

— limit of structural damage (limit of the overall deformations and other effects such as spalling, corrosion, charring occurring during the heating and the cooling phases) to allow reparability of building after fire (re-serviceability or reusability limit state).

For separating elements, they include:

— limit on the temperature rise of the unexposed surface, (+140 °C average, +180 °C max);

— limit on the leakage of hot gases through gaps created in the element (movement of gap gauge, cotton wool pad);

— limit on the thermal radiation from the unexposed face, (for escape routes 3 kW/m^2).

The human skin can only tolerate a certain level of heat flux for a certain time. The higher the incident heat flux level the shorter the tolerable exposure time. Some typical critical values are presented in Table 1.

Table 1 — Examples of human tolerance and physiological damage from exposure at ambient temperature to various levels of incident radiant heat flux from a remote emitter

Incident radiant heat flux kW/m^2	Physiological Effect
1.0	Maximum for indefinite tolerability
4.0 - 5.0	Sufficient to cause pain to personnel if unable to reach cover in 20 seconds. Blistering of the skin (second degree burns) is likely, 0 % lethality
10.0	Intolerable pain after 12 seconds
12.5 - 15.0	1 % lethality in 1 minute, first degree burns in 10 seconds
25.0	100 % lethality in 1 minute; significant injury after 10 seconds
35 - 37.5	100 % lethality in one minute; 1 % lethality in 10 seconds
41.8	Skin necrosis to 0.05 mm depth after 2 seconds

More detailed information is given in the publication Risk-Informed, Performance Based Industrial Fire Protection (ISBN 1-882194-09-8).

Other criteria may be based upon the incident heat flux to cause ignition on different types of materials as shown in Table 2.

Table 2 — Incident radiant heat flux from a remote emitter for ignition after 10 minutes exposure at ambient temperature

Material	Incident radiant heat flux kW/m^2
Polystyrene	18
Polymethyl methacrylate	18
Polyethylene	20
Polypropylene	20
Paper	20
Polyvinyl chloride	21
Nylon	29
Wood	32

The criteria may also depend upon the ability of certain types of products to withstand specific temperatures as presented in Table 3. These are indicative only.

Table 3 — Effect of temperature on selected materials

Material	Typical Examples	Damage Conditions	Approximate Temperature °C
Polystyrene	Thin walled food containers, foam, light shades, handles, curtain hooks, radio casings	Collapse Softens Melts and flows	120 120 - 140 150 - 180
Polyethylene	Bags, films, bottles, buckets, pipes	Shrivels Softens and melts	120 120 - 140
Critical temperatures may be dependent upon the rate of heating. in particular, glass products are also dependent upon the impact of water as well as the framing and glass condition.			

Table 3 *(continued)*

Material	Typical Examples	Damage Conditions	Approximate Temperature °C
Polymethyl meth-acrylate	Handles, covers, skylights, 'glazing'	Softens Bubbles	130 - 200 250
PVC	Cables, pipes, ducts, linings, profiles, handles, house ware, toys, bottles	Degrades Fumes Browns Chars	100 150 200 400 - 500
Cellulose	Wood, paper, cotton	Darkens	200 - 300
Paint surface- resin-ous or oil based	-	Deteriorates Destroyed	100 250
Annealed soda-lime-silica glass	Window glass, doors and internal glazing	Cracking due to thermal gradients leading to falling out Softening pointWorking point Practical melting point	Thermal gradient typically 160°C 720°C 1010°C
Wired glass	Window glass, doors and internal glazing	Cracks as for annealed but wires ensure pieces stay in place	
Toughened (or tem-pered) soda-lime-silica glass	Impact safety glazing	Subject to unpredictable cata-strophic thermal shock failure If integrity retained, softening as above	Thermal gradient typi-cally in range 150°C to 280°C (see note)
Laminated soda-lime-silica glass	Security and safety glazing, with pvb interlayer	Glass layers crack and behave as above Organic interlayer starts to degrade leading to smoking and ignition	Starts from ~180°C accelerating from ~300°C onwards

Critical temperatures may be dependent upon the rate of heating. in particular, glass products are also dependent upon the impact of water as well as the framing and glass condition.

3 Design process

In order to evaluate the performance of a structure or a part of it, the assessment has to be carried out in three stages:

Stage 1: Analysis of the thermal actions/exposure - fire model

Stage 2: Analysis of the heating rate and temperatures attained by the structural components - heattransfer model

Stage 3: Analysis of the mechanical/load bearing performance of the member/s - structural model

These are described as follows:

3.1 Fire model

The thermal exposure (design fire) is generally described by a temperature-time relationship but can also be described by a time dependent – incident radiant condition, which could be simulated as by a temperature-time relationship. The fire model can therefore be a nominal (furnace) fire, or, a fire simulating a real scenario, or even an experimental fire.

The first stage of fire (pre-flashover phase) is generally regarded the most critical for human life since during this stage smoke and toxic gases are produced. When dealing with structural fire resistance, this phase has in the past, been ignored, since the temperatures reached although critical for human beings,

are generally too low to seriously affect the mechanical behaviour of a structure. However, with the use of aluminium, structural plastics and resins becoming more widely employed in situations where their performance in fire can be critical, the pre-flashover fires should not be ignored. Aluminium and/or alloys virtually lose all their strength at around 400 °C. Structural plastics can char in a very similar manner to timber at temperatures below 300 °C.

In the future it is expected that pre-flashover fires may be simulated into a furnace test in a standardised way or as incident radiant heat flux with time.

However, when a fire occurs, it is not obvious that it will reach such a severity that it will endanger a load-bearing structure. A wide range of factors such as detection, automatic extinguisher system, fire brigade action etc., need to be taken into account (generally by using a probabilistic approach) in order to provide a more representative evaluation of the fire exposure conditions and resulting structural fire response.

The design fire used to assess the fire resistance assessment of a structural member/s can be based upon:

— A nominal fire, which is expressed by a well - defined temperature-time relationship. This would be typically a Standard furnace test upon which national Regulations are set, although it is primarily used for ranking of products and systems rather than reflecting reality.

— A natural fire, based upon a simple formula or a set of temperature-time curves, taking into account the main parameters that influence the time temperature response within the compartment. These are often referred to as single zone fire models or parametric fires and would be used in simple easily defined compartment geometries.

— A fire determined using complex numerical calculations such as multi-zone models or **C**omputational **F**luid **D**ynamics. This type of advanced analysis would be required in very large compartments, compartments with complex geometries and possibly high and irregular ceilings.

For a more comprehensive review of design fire scenarios and design fires reference should be made to ISO/TS 16733.

3.2 Heat transfer model

The heat transfer analysis is carried out to determine the temperature rise and distribution within the structural members. Thermal models are based on the acknowledged principles and assumptions of the theory of heat transfer. They may present various levels of sophistication according to the assumptions and needs. Models vary in complexity and may be used simply to determine a uniform temperature distribution, or, more complex temperature distributions in which thermal gradients may be calculated in 1, 2 or 3 directions.

The formulation of transient state heat conduction problems differs from that of steady cases in that the transient problems involve an additional term representing the change in the energy content of the medium with time. This additional term appears as a first derivative of temperature with respect to time in the differential equation, and as a change in the internal energy content during Δt, in the energy balance formulation. The nodes and the volume elements in transient problems are selected as in the steady case. For convenience, it is assumed that all heat transfer is into the element.

The energy balance on a volume element during a time interval Δt can be expressed as:

$$
\begin{pmatrix}
\text{Heat transfer into the} \\
\text{volume element from} \\
\text{all of its sides during} \\
\text{a time interval } \Delta t. \\
\sum \dot{Q}
\end{pmatrix}
+
\begin{pmatrix}
\text{Heat generated within} \\
\text{the volume element} \\
\text{during a time} \\
\text{interval } \Delta t. \\
G
\end{pmatrix}
=
\begin{pmatrix}
\text{The change int the} \\
\text{energy content of} \\
\text{the volume element} \\
\text{during } \Delta t. \\
\Delta E / \Delta t
\end{pmatrix}
$$

or

$$\sum \dot{Q} + G_{element} = \Delta E_{element} / \Delta t$$

The rate of heat transfer $\dot{Q}$ normally consists of conduction terms for interior nodes, but may involve heat flux (convection and radiation)for boundary nodes. The sum of Q is zero except at the boundaries.

Materials that incorporate free moisture should consider the effect of migration of moisture through the system in order to provide an accurate representation of the thermal distribution with time. This can be handled in the thermal analysis by incorporating mass transfer in the model. Where this is used, additional information can be provided on pressure field due to steam being produced and also to provide useful information on materials that are subject to the phenomena of spalling.

3.3 Structural model

The structural analysis/model used very much depends upon the structural form that is being analysed and can broadly be described as follows and shown in <u>Figure 3</u>.
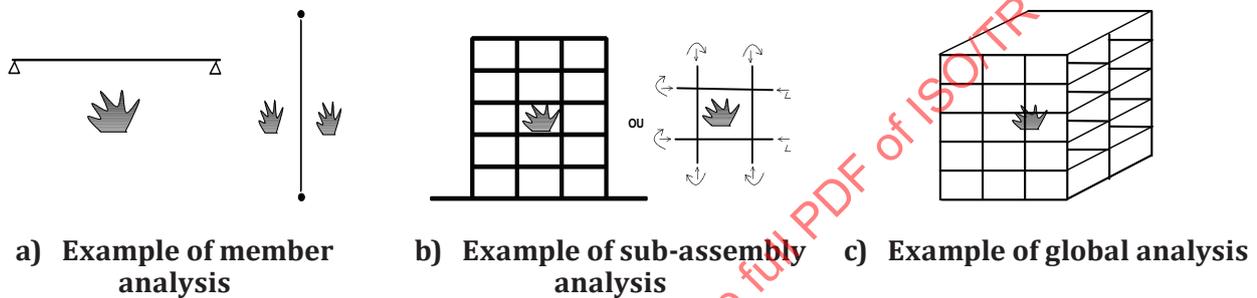

| a) Example of member analysis | b) Example of sub-assembly analysis | c) Example of global analysis |

Figure 3 — Examples of types of analyses

Single member analysis, (e.g. beams, columns, floors, walls) are usually considered when verifying standard fire resistance requirements although they can be considered in real fire scenarios. The restraint conditions at the supports that exist at the beginning of a test (time = 0) generally remain unchanged throughout the fire exposure period. Only the effects of thermal deformation resulting from temperature gradients created through the cross-section need to be considered. Thermal expansion effects are usually ignored.

Sub-assembly analysis (e.g. sub frames and assembly of members). The conditions set at the beginning of a test will change upon heating. In particular, forces that are developed either through expansion or contraction (during cooling) will be considered as well as load transfer to other parts of the structure when one or more members loose their load bearing capacity. However, the effects of restraint from the rest of the frame particularly in respect of expansion effects and local failure, are only considered in a minor way. Sub-frame analysis can be carried out under both nominal and real fire scenarios.

Global structural analysis (of the whole structure in which a fire occurs). This takes into account heat transfer conditions, relevant failure modes, temperature-dependent material properties, stiffness as well as effects of thermal expansion effects where relevant. Load distribution is generally considered unchanged during the whole of the fire exposure period. While a global analysis is primarily carried out under natural fire heating conditions it can also be applied under furnace heating conditions although the effects of the cooling phase on the structural response would not normally be considered.

3.4 Combination models

Use of the models for fire, heat transfer and structural analysis, have to be considered in terms of the level of sophistication required. There is little point in conducting exact heat transfer analysis if when it comes to the structural analysis a very coarse approach is adopted unless it can be shown an insensitive coarse model is sufficiently accurate within the context of the outputs required.

There are some combinations of thermal and structural analysis where it would be impracticable to carry out other than for calculation purposes. Figure 4.
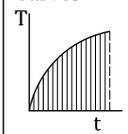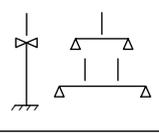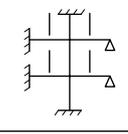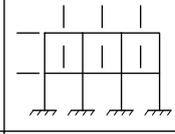
Model for structure	S_1	S_2	S_3
Model for thermal exposure	Element	Substructure	Complete structure
H_1 Nominal temperature-time curves	test or calculation (deterministic)	calculation, exceptionally testing (deterministic)	
H_2 real fire	calculation (probabalistic)	calculation (probabalistic)	calculation (probabalistic) in special cases and for research

Figure 4 — Combination of thermal and structural analysis

Thermal Model H_1 describes the thermal exposure according to the standard fire resistance test of structural elements as specified in ISO 834 and in the corresponding national standards, or according to some other nominal or characteristic temperature-time curve. A fire design based on this thermal exposure, represents the internationally prevalent situation for load bearing and separating structural elements. It would be applied to single elements or simple sub-frames.

Thermal Model H_2 describes a thermal exposure based on a simulated real fire and either computed by solving the energy and mass balance equations of the compartment fire or determined from some systematized design basis. For example, Eurocode 1: Actions on structures exposed to fire, presents a set of parametric equations. These are very similar to the gas temperature-time curves based upon energy and mass balance equations of the fully developed compartment fire for which computer codes are available (SFIRE, COMPF-2 and BRAND). These models can be applied to single elements, sub-frames as well as to the complete structure. Furnace tests are currently being considered that represent the heating conditions of occupancy related fires scenarios.

Structural Model S_1 comprises single structural elements, e.g. beams, columns, walls, floors, and roofs. The model then may simulate either a structural element, which behaves as a single element in the real structure, or an element, which in reality acts together with other elements of the complete structure, but is cut out of this and described by simplified end conditions in the fire analysis.

Structural Model S_2 refers to a substructure, which approximately describes the mechanical behaviour of a part of the complete load bearing system of the building. Compared to the real structure, a substructure is analysed with simplified boundary conditions at its outer ends or edges.

Structural Model S_3 describes the mechanical behaviour of the complete load bearing structure of the building acting as, for instance, a two or three dimensional frame, a beam-slab system or a column-beam-slab system.

In the matrix presented in Figure 4, the thermal exposure models and the structural models are combined in the sequence of improved idealization. In principle, each element in the matrix then represents a particular design procedure. The matrix can therefore be considered as a type of classification system for methods of structural fire engineering design. It is, however, evident that not all models can be used in all combinations and the aim should be to provide a sensible pairing at each level of advancement. In

the matrix, reference is made to these aspects. In principle, a structural fire engineering design offers a problem oriented choice for the combination of the thermal exposure model and the structural behaviour model and the final choice may also depend on national preferences, the complexity of application and the particular design situation.

3.5 Material properties

The material properties required for thermal and structural models including any fire protection materials can be broadly divided into two areas and generally may be used during heating under standard furnace test or representative occupancy related characteristic fires. They are not necessarily appropriate for structural analysis during the cooling phase.

3.5.1 Thermo – physical properties

The solving of the equations of transient heat flow to and within a fire exposed structure, requires information on the following properties for the structural materials and insulation/protection where appropriate

— emissivity of the fire exposed surfaces of the structure (a value of 1 is normally assumed for any applied fire protection),

— thermal conductivity of the structural materials and the fire protection,

— specific heat of the structural materials and the fire protection,

— thermal energy due to phase changes at various temperature levels of the structural materials and for some protection materials,

— rate of internally generated heat in the structure and fire protection,

— thermal expansion/contraction of the structural materials,

— density of the structural materials and fire protection.

For structures of combustible material, additional information on the rate of charring is required.

The properties must be known as a function of temperature for the heating as well as the subsequent cooling-down phase of the compartment fire. More advanced analysis, consisting of a solution of inter-related heat and mass transfer equations, requires information on a considerable number of additional properties such as:

— permeability of the structural materials,

— diffusion coefficient of adsorbed water and vapour in the structure,

— void fraction of the structure,

— equilibrium water content in the structure,

— crystalline water content in the structure,

— reaction rate and heat of reaction in the process of pyrolysis for structures of combustible materials,

— heat of reaction at the oxidation at the surface of structures of combustible material, and

— specific heat and dynamic viscosity of water vapour and volatile pyrolysis products.

For most fire protection materials the thermal properties are significantly different in the cooling phase.

3.5.2 Mechanical properties

A reliable calculation of the mechanical behaviour of a fire-exposed structure based upon the transient temperature state requires validated models for the mechanical behaviour of the materials involved

within the temperature range associated with fires. These include mathematical relationships with respect to temperature that describe:

— elastic modulus,

— compressive strength,

— tensile strength,

— shear strength, including strength of shear connectors,

— torsional strength, and

For reinforced structures: strength with respect to bond and anchorage, as a function of temperature and, when relevant, stress history.

For a determination of the deformation behaviour and the ultimate load with respect to instability failure of fire-exposed structures and structural members, additional information is required for these properties:

— stress-strain relationship,

— steady-state and transient creep,

— steady-state and transient shrinkage,

— thermal expansion,

— relaxation

In structural models, it is not unusual to find that the material model for the mechanical behaviour is specified by temperature-dependent stress-strain curves that either neglect or indirectly include the creep strains and transient strains. The stress-strain curves are determined either from small-scale material tests or from full-scale tests on that type of load-bearing structure, for which the computational procedure is developed.

Fundamental parameters for determining the mechanical material properties at elevated temperatures are the rate of heating, load application and the control of strain. Practically, information on the material models can be referred to different testing regimes as shown.
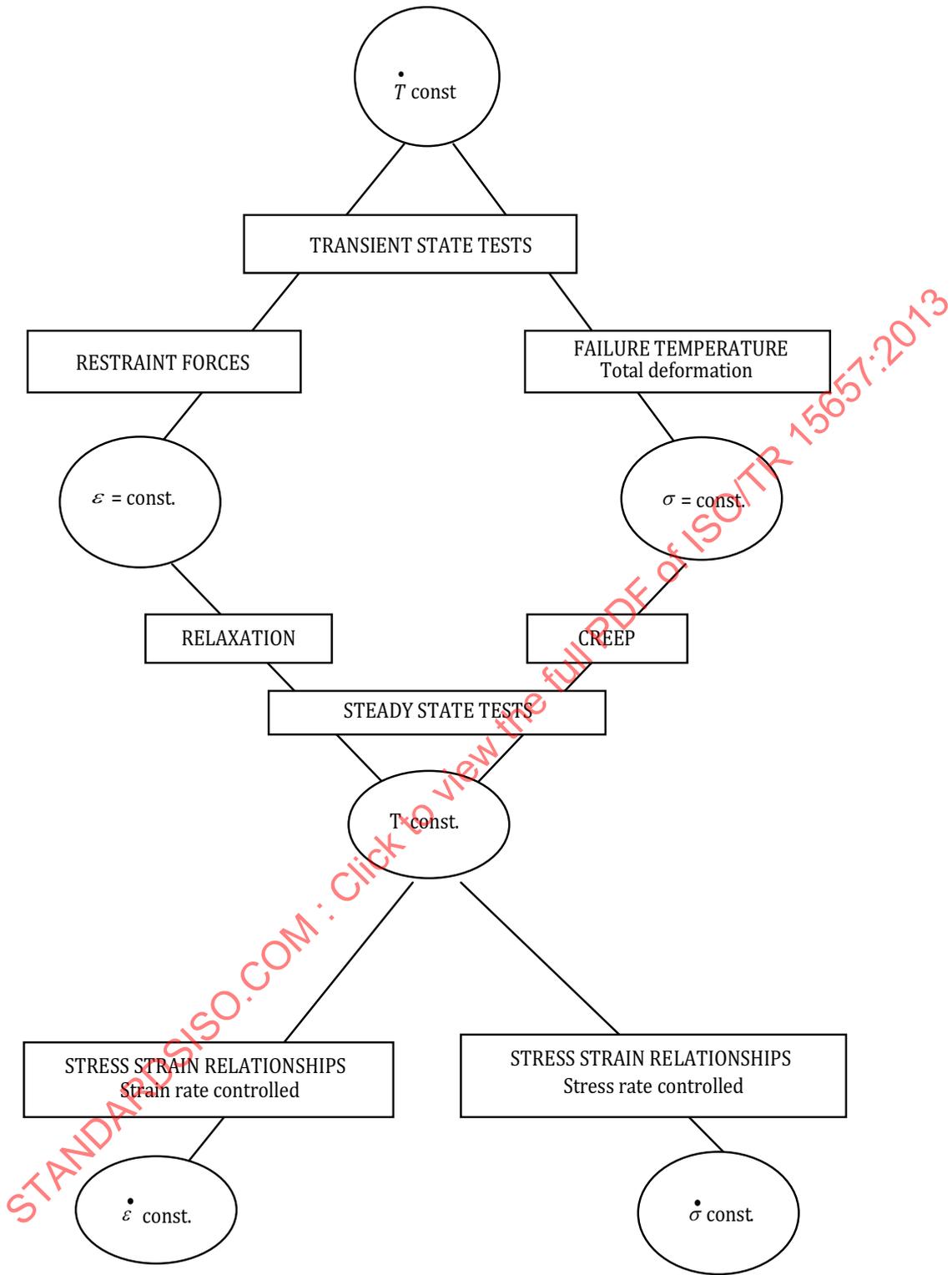
Figure 5 — Various testing regimes for determining the mechanical properties of materials at elevated temperatures

Much of the information used in either thermo-physical, and mechanical models are given in the Eurocodes 2 - 6 and 9, see Annex A. Other data are given in CIBSE (Chartered Institute for Building Services Engineers) Guide E (UK) and SFPE Handbook on Fire Protection Engineering.

For separating elements and fire protection materials, similar thermo-physical and mechanical properties are required that cover for example: gypsum, calcium silicate, mineral wool, vermiculite cement etc.

Material properties are required over a range of temperatures depending upon the environment under which they may be used or the exposure conditions. For building fire scenarios and hence furnace tests temperatures are unlikely to exceed much above 1200 °C. The exception would be the heating conditions that relate to tunnel fires whereby some materials may be exposed to temperatures up to 1350 °C.

The design values of the material properties are obtained by using partial safety factors. Design values of thermal and mechanical material properties $X_{fi,d}$, are defined as follows:

Thermal properties for thermal analysis:

If an increase of the property is favourable for safety then:

$$X_{fi,d} = X_{k,\theta} \times \gamma_{M,fi} \tag{3.1}$$

If an increase of the property is unfavourable for safety then:

$$X_{fi,d} = \gamma_{M,fi} \times X_{k,\theta} \tag{3.2}$$

where;

$X_{fi,d}$ is the design value of thermal and mechanical property

The X can be any property of interest for thermal or mechanical calculations.

The X is meant to be substituted with properties like λ (thermal conductivity), C (specific heat), E (modulus of elasticity), f (strength), ρ (density), w (moisture content).

The subscripts have the following meaning:

fi =   Fire design

d =   Design

The use of X is a general way of explaining the influence of a partial coefficient or factor on the property of interest. It depends on the type of property whether an increase of the property is favourable for safety. An increase in λ (thermal conductivity) is not favourable for safety, where an increase in f (strength) is favourable.

Strength and deformation properties for structural analysis:

$$X_{fi,d} = k_\theta X_k / \gamma_{M,fi} \tag{3.3}$$

where;

$X_{fi,d}$ is the characteristic value of a material property in fire design, generally dependent on the material temperature,

X_k is the characteristic value of a strength or deformation property (generally f_k or E_k) for normal temperature design,

k_θ is the reduction factor for a strength or deformation property, $(X_{k,\theta}/X_k)$, dependent on the material temperature,

$\gamma_{M,fi}$ is the partial safety factor for the relevant material property, for the fire situation

Proposals for partial safety factors for various materials (according to Structural Eurocodes 2-6 and 9) are assumed to be 1.0 for both the thermal and mechanical properties for all materials.

4 Fire models

Several models can be used to describe the thermal actions upon a structure. A number of examples are illustrated in Figure 6.
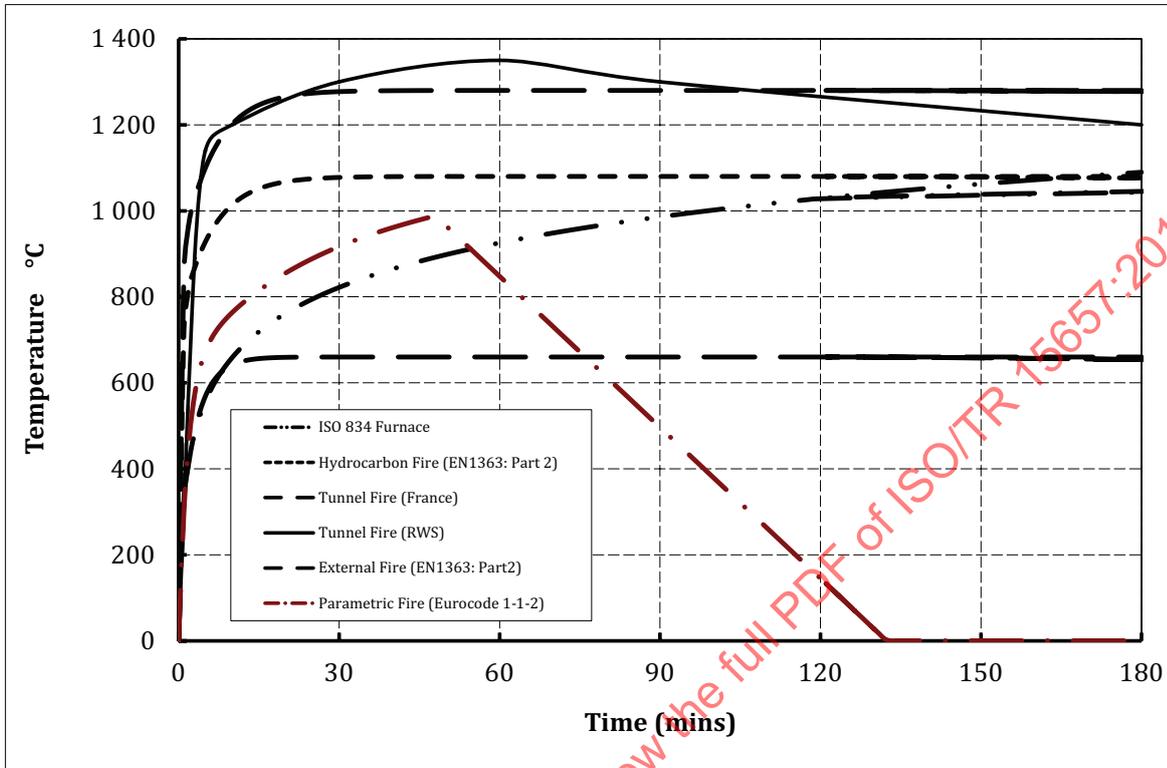

Figure 6 — Fire curves

The different types of fire generally fall within one of the following categories. These are:

— Standard Furnace (nominal) heating curves given, for example, in ISO 834

— Simplified formulae representing a natural fire or a set of temperature - time curves

— Steady-state fires

— Complex models that describe the spatial behaviour within a compartment that numerically describe the fire process

— Experimental fires

4.1 Standard (nominal) fires

There are four nominal temperatures - time furnace heating curves given as a function of time (t) and temperature (θ_g):

Cellulosic curve (ISO 834-1)

The standard temperature-time curve often referred to as the cellulosic curve, is given by the relationship:

$$\theta_g = 20 + 345 \log_{10}(8t + 1) \qquad [°C]$$

(4.1)

External fire curve (currently EN 1363-2)

To characterize less severe fires immediately outside enclosures or emanating from within the building e.g. the condition of flames issuing from adjacent windows, the temperature/time relationship is given by

$$\theta_g = 660(1 - 0.687e^{-0.32t} - 0.313e^{-3.8t}) + 20 \qquad [°C]$$

(4.2)

Hydrocarbon fire curve (Currently EN 1363-2)

The hydrocarbon temperature - time curve which, realistically represents a hydrocarbon fire is given by:

$$\theta_g = 1080(1 - 0.325e^{-0.167t} - 0.675e^{-2.5t}) + 20 \qquad [°C]$$

(4.3)

Tunnel fire curves

In 1979 the RWS-curve originated from tests carried out in a model tunnel in which the temperatures attained 1350 °C after 60 minutes. The RWS-curve was developed by the Rijkswaterstaat, Ministry of Transport in the Netherlands and was based on the assumption that in a worst case scenario, a fuel, oil or petrol tanker fire with a heat release of 300 MW could occur and last for up to 120 minutes.

The primary difference between the RWS and the Hydrocarbon heating conditions is that the hydrocarbon curve is based on the temperatures that would be expected from a fire occurring within a relatively open space, where some dissipation of the heat would occur. In contrast, the RWS curve is based upon the conditions experienced by a fire occurring in an enclosed area, such as a tunnel, where there is little or no opportunity of heat dissipating into the surrounding atmosphere.

The RWS curve simulates the initial rapid growth of a fire using a petroleum tanker as the source, and the gradual drop in temperature reflects the reduction in fire load as it is burnt off. It has been used as a Standard for the protection of tunnels in the Netherlands since the 1980s.

The heating portion of the RWStunnel curve can be obtained by replacing 1080 °C in the hydrocarbon curve by 1350 °C.

France (HCM) and Germany (RABT-ZTV for trains and cars) also have tunnel fire curves which are illustratedin [Figure 6](#).

Smouldering Fire:

In addition, a slow heating curve is also described in which the temperature within the furnace attains 345 °C after 20 minutes and then joins the cellulosic curve. This is not used as a thermal action for design purposes, but may be called upon for certain reactive fire protection materials, which rely upon a chemical/physical change in order to function as an insulator.

However, where fire safety devices rely upon only the action of hot smoke to function it is recommended until such time when there is an internationally agreed temperature/time curve the performance of devices are evaluated using the smouldering fire curve described in EN 1363-2 by the following equation:

For $0 < t \le 21$

$$T = 20 + 154t^{0.25} \qquad [°C]$$

(4.4)

For $t > 21$

$$\theta_g = 20 + 345 \log_{10}\{8(t - 20) + 1\} \qquad [°C]$$

(4.5)

4.2   Natural fires

The parametric fire can be used for simulating the behaviour of post flash-over fires and can be used to represent characteristic occupancy related fires. This is an area of current research in which characteristic fires are being considered for standardization.

Since the fire consider the whole compartment has reached post-flashover and that there is no variation in temperature across the compartment in any direction, it is referred to as a Single Zone fire.

For compartment fires the temperature - time history of the entire fire process is given by the relationship:

$$\theta_g = 20 + 1325(1 - 0.324e^{-0.2t^*} - 0.204e^{-1.7t^*} - 0.472e^{-19t^*}) \qquad [°C]$$

(4.6)

where:

θ_g is the gas temperature in the fire compartment, °C

$$t^* = t \cdot \Gamma \qquad [h]$$

(4.7)

with;

t = time   [h]

$$\Gamma = [O/b]^2/(0.04/1160)^2 \qquad [-]$$

(4.8)

O is the opening factor and is given by:

$$A_v h^{1/2}/A_t \qquad [m^{1/2}]$$

(4.9)

where:

A_v is the area of vertical openings   [m^2]

h is the weighted mean height of the vertical openings   [m]

A_t is the total area of the enclosure (walls, floor and ceiling including the openings)   [m^2]

Using Γ = 1 in Formula (5.7) gives the standard (ISO) time-temperature curve, and using Γ = 50 and replacing 1325 by 1080, approximates to the Hydrocarbon fire.

In the Code, the limits of 0.02[O[0.20 are observed. However, the UK considers the opening factor can been extended down to 0.01 m$^{1/2}$ and can be applied to buildings with compartment floor areas greater than 500 m^2.

In the above equation, $b = \sqrt{(\rho c \lambda)}$.

In which b is the thermal absoptivity of the total enclosure and has now been extended to cover a wider range of compartment types with:

$$100 \leq b \leq 2200 \qquad [\text{J/m}^2\text{s}^{1/2}\text{K}]$$

(4.10)

The lower value would be representative of a compartment or building with a controlled environment and clad with lightweight insulation typically 6" (150 mm) thick whereas the upper value is representative of a very poorly insulated structure such as a dense concrete and un-insulated steel sheeting, e.g. unheated storage facility.

The Code recognizes the importance of the thermal properties of the compartment walls/floor/ceiling and is represented together with consideration of walls, which comprise two or more layers

The maximum temperature within the compartment is given by:

$$t_{\max} = \max[(0.2 \times 10^{-3} \times q_{t,d}/O); t_{\lim}] \qquad [\text{h}]$$

(4.11)

where:

$q_{t,d}$ is the design fire load density and should obey the following limits: $50 \leq q_{t,d} \leq 1\,000$ MJ/m²

$t_{\lim}$ is given in hours.

The fire growth rate is taken into account in which $t_{\lim}$ = 15 min, 20 min, and 25 min is applied for fast, medium and slow growth rates respectively.

To account for different values of b representing the walls, ceiling and floor, $b = \sqrt{(\rho c \lambda)}$ is introduced as:

$$b = \left(\sum \left(b_j A_j \right) \right) / (A_t - A_v) \qquad [\text{J}/\text{m}^2\text{s}^{1/2}\text{K}]$$

(4.12)

where:

A_j is the area of enclosure surface j, openings not included

b_j is the thermal property of enclosure surface j.

The temperature-time curves in the cooling phase are given by;

$$\theta_g = \theta_{\max} - 625(t^* - t^*_{\max} \cdot x) \text{ for } t^*_{\max} \leq 0.5 \qquad [^\circ\text{C}]$$

(4.13)

$$\theta_g = \theta_{\max} - 250(3 - t^*_{\max})(t^* - t^*_{\max} \cdot x) \text{ for } 0.5 < t^*_{\max} < 2 \qquad [^\circ\text{C}]$$

(4.14)

$$\theta_g = \theta_{\max} - 250(t^* - t^*_{\max} \cdot x) \text{ for } t^*_{\max} \geq 2 \qquad [^\circ\text{C}]$$

(4.15)

where:

$x =$ 1.0 if $t_{\max} > t_{\lim}$, or $x = t \lim \cdot \Gamma / t^*_{\max}$ if $t_{\max} = t_{\lim}$

A series of parametric fires is given in Figure 7 (fire load = 140 MJ/m², b = 1160, opening factor O from 0.04 m$^{1/2}$ to 0.30 m$^{1/2}$).
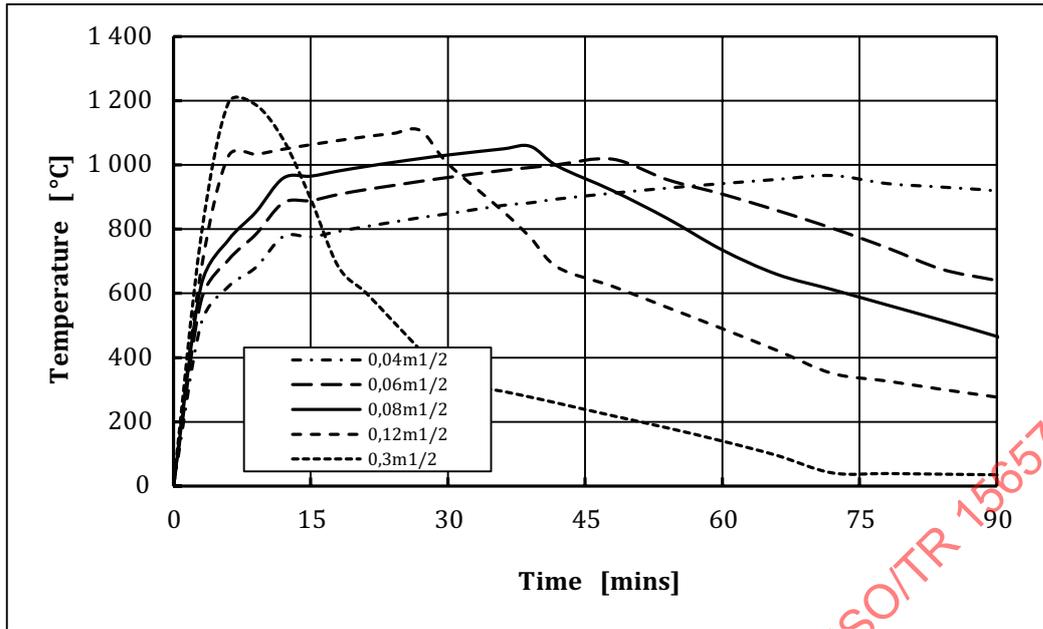
Figure 7 — Set of parametric fires

4.3 Numerical simulation of natural fires - Zone models

Zone models and field models generally are deterministic models. They can be used to solve problems in a number of categories, i.e. smoke and heat transport in enclosures, detector/sprinkler activation and evacuation of humans. They can provide very detailed simulations of complex fire scenarios and for this reason require considerable CPU.

The simplest representation of a compartment fire is a **Single Zone** model, which is generally applied to post flashover conditions. Homogeneous properties of the gas are assumed in the compartment such as the temperature, optical properties, chemical composition.

The temperature may be calculated by a heat balance approach considering the resolution of mass and energy conservation equation:

$$I_C = I_L + I_W + I_R + I_B \qquad [kW]$$

(4.16)

where:

I_C is the heat released during combustion

I_L is the heat removed due to replacement of hot gases by cold air

I_W is the heat loss to boundary surfaces

I_R is the heat dissipated by radiation through the openings

I_B is the heat stored in the gas volume (usually ignored)

The exchange of mass with the internal gas comes from the external gas (by openings) and the fire (pyrolysis rate), whereas the exchange of energy with the internal gas is calculated with respect to the surrounding surfaces, the fire and the openings.

The quick response of this model and its simple equations give an advantage to the one-zone model and it is a helpful tool to estimate the temperature in a compartment after flashover has been achieved. Examples have already been given in Figure 7.

The **two-zone model** is based on the assumptions of accumulation of combustion products in a layer beneath the ceiling, with a horizontal interface. In this upper layer, one assumes uniform characteristics of the gas. Different zones are defined: the upper layer, the lower layer, the fire and its plume, the external gas and walls. The exchanges of mass, energy (and chemical species) are calculated between these different zones.

Zone models contain usually sub-models referring to processes in the gas zones and various transport and combustion processes. Therefore, the computer code contains subroutines dealing with:

— conservation equations for the gas zones

— source term sub-models

— mass transfer sub-models

— heat transfer sub-models

— embedded sub-model

The application of this type of model is mainly in pre-flashover conditions, and is used to evaluate the propagation of smoke in buildings, and estimate the life safety in terms of tenability criteria as a function of temperature, radiative flux, optical density and toxic gas concentration.

The general criteria for assuming the occurrence of flashover are:

— 500 °C to 600 °C in the upper layer,

— 25 kW/m² for radiation to the floor,

— flames emerging from window.

Field models or CFD models (computational fluid dynamics models) are the most sophisticated deterministic models for simulating enclosure fires. Field models incorporate sub-models for turbulence, heat transfer and combustion.

The CFD modelling technique is based on a complete, time-dependent, three dimensional solution of the fundamental conservation laws. The volume under consideration is therefore divided into a very large number of sub-volumes. The basic laws of mass, momentum, and energy conservation are applied to each of the sub-volumes.

The governing conservation equations for mass, energy, and momentum contain as further unknowns the viscous stress components in the fluid flow. Substitution of the viscous stress components into the momentum equation and solving them is central to any CFD code (so called Navier-Stokes equations).

Two cases of field models exist:

Direct numerical simulations (DNS)

The basic equations are solved without averaging, but such codes need a very short time and spatial step in order to simulate all time and spatial scale coming from the turbulent and the chemical processes. DNS require particularly powerful computers and are used for academic studies or confined to simple applications. The large eddy simulation (LES) technique is an example where the most realistic simulation of fire-induced flows can be performed.

Reynolds-averaged Navier Stokes (RANS)

The basic equations are pre-averaging on very short time scale, and use a turbulent model to take into account the short spatial scales. The most frequently model used is a second order closed $k - \varepsilon$ model.

All flows encountered in engineering practice become unstable above a certain Reynolds number and are said to be turbulent. The velocity fluctuations associated with turbulence give rise to additional stresses on the gases, the so-called "Reynolds-stresses", described by the Reynolds equations. A direct solution of the time dependent equations of fully turbulent flows at high Reynolds numbers require extremely fine geometric grids to describe the temperature and velocity (and chemical species concentration) and therefore extremely small time steps to describe all the points in the compartment.

Certain assumptions must therefore be made to avoid the need to predict the effects of each and every eddy in the flow.

The k-ε model is a turbulence modelling approach that is based on the time-averaged Reynolds equations. Two transport equations (partial differential equations) are solved, one for the turbulent kinetic energy, k, and another for the rate of dissipation of turbulent kinetic energy ε. The equations used contain a number of empirical constants, determined from experimental results. A number of variations of the k-ε model exist; the so called standard k-ε model is widely used in CFD-codes. One of the main drawbacks of this model is that the eddy viscosity is assumed to be identical for all the Reynolds stresses, so that the turbulence has no preferred direction.

The mass of air entrained into a fire plume controls to a considerable degree the process of smoke filling, the concentrations and temperatures in the hot layer, and the combustion in the flame. The standard k-ε model does not model gravitational forces correctly. Gravitational forces apply only in the vertical direction. To model plume entrainment correctly the standard k-ε model can be partly amended by using buoyancy modifications. In this enhanced k-ε model the constants in the Reynolds stress equation have been changed in order for the plume to widen with the height as it does in reality. However, this has adverse effects in other regions, such as in the flame extensions under ceilings, i.e. the ceiling jet. Therefore further work is clearly needed on the turbulence models used in CFD codes to fit experimental data better.

CFD modelling is complex and a minor change in the input data may have an enormous influence on the output data. Nevertheless, CFD modelling may in some cases, be the only way to tackle particular design problems.

4.4 Heat flux to the structure

To calculate the thermal action upon structural members from fires which are defined in terms of a temperature-time relationship the following equation can be used to obtain the net heat flux ($\dot{h}_{net}$) from the convective and radiative components of heat transfer:

$$\dot{h}_{net} = \dot{h}_{net,c} + \dot{h}_{net,r} \quad [\text{W}/\text{m}^2] \tag{4.17}$$

Where the convective heat flux component is given per unit surface area of the structural member by:

$$\dot{h}_{net,c} = \alpha_c \cdot (\theta_g - \theta_m) \quad [\text{W}/\text{m}^2] \tag{4.18}$$

In which:

α_c is the coefficient of heat transfer by convection equal to:

- 25 W/m^{2}K for standard and external fire curve,
- 50 W/m^{2}K for hydrocarbon fire curve,
- 35 W/m^{2}K for "natural" fires,
- 9 W/m^{2}K on the unexposed side of separating members.

θ_g is the gas temperature of the environment around the member   [°C]

θ_m is the surface temperature of the member   [°C]

The radiative heat flux component per unit surface area is given by:

$$\dot{h}_{net,r} = \Phi \cdot \varepsilon_m \cdot \varepsilon_f \cdot \sigma[(\theta_r + 273)^4 - (\theta_m + 273)^4] \qquad [\text{W/m}^2] \qquad (4.19)$$

where:

Φ is the configuration factor and is assumed to equal 1.0 without further consideration [-]

ε_m is the emissivity of the material in which a default value of 0.8 is used without further information [-]

ε_f is the emissivity of the fire which is taken as 1.0 without any further consideration [-]

θ_r is the radiation temperature of the environment of the member [°C]

θ_m is the surface temperature of the member [°C]

N.B in Eurocode 1-1-2 Formula (4.19) includes a term ε_f which is the emissivity of the fire and is taken as 1.0 without any further consideration. For steel, some countries use a value of 0.8 for the emissivity of steel and then apply a correction factor of 0.9 in Formula (5.1), (sometimes referred to as the shadow factor) that enables the calculated temperature rise to align with measured data. Other countries do not agree with this principal and adopt a value of ε_m = 0.7 without the correction. Both methods give similar results.

In situations where radiation from the fire passes through a glazed system, the extent of radiation seen by the structural members is very much reduced compared with radiation emitting through an open window.

Radiation from Panes of Glass in Fire:

The transmissivity of glass is dependent on wavelength, which depends upon the glass thickness and the trace element composition of the glass. In a fire, the glass is exposed to electromagnetic radiation on the fire side. This radiation has a spectrum, which means that the energy transferred in various wavelength intervals may be different.

The radiation from a fire is partly in the interval from 350 nm to 780 nm, which is visible light. This is why the flames are visible. However, the majority of the energy radiated from a fire is in the infrared, i.e. wavelengths longer than 780 nm.

The transmissivity coefficient of glass for infrared radiation is very low. In other words, the electromagnetic energy is not radiated through to the full extent. However, the glass pane itself becomes hot by radiation and by convection and, therefore, the glass pane temperature increases. The glass pane itself then starts radiating electromagnetic radiation in wavelengths higher than 780 nm. The radiation component transmitted from the furnace through the glass is approximately 10 %. The glass acts as a radiation screen for the other 90 %. For this reason glass does not provide a great resistance against heat transfer.

As the glass itself starts emitting radiation, a thermal exposure may be received at a certain distance from the glass pane. If the glass is coated with a heat reflective coating on the exposed side, then the heat flux received on the unexposed side can be strongly reduced. Some fire resisting glasses can provide a heat flux reduction of up to 50 % due to heat reflective coatings.

It needs to be recognized that the behaviour of the coating itself is also wavelength dependent, and therefore, the coating is selective with respect to radiative heat transfer in various wavelength intervals. These are often used to control the internal environment in buildings.

The glasses that meet integrity and insulation performance are of two types: intumescent laminated and cast-in-place gels. They are different and function differently in a fire. The first – intumescent laminated – is composed of a hard inorganic glassy layer between plates of standard annealed soda-lime-silica glass. Real fire experience is available to illustrate that such intumescent laminates are capable of resisting extreme intense fire conditions. The gel type has a fluid layer between two plates of toughened glass and

depends for its action in fire on its high water content. The deterioration mechanism is different and can depend sensitively on failure of the toughened glass plates.

In both cases, insulation performance serves to reduce heat levels by conduction, convection and radiation to low tolerable levels. The same technologies can also be used to give enhanced integrity performance in integrity only formulations in which the intumescent layer enables the system to be more tolerable to marked changes in temperature rise and non uniform distribution.

5 Heat transfer models for temperature calculations

The second stage in determining the behaviour of structural members in fire is to establish their temperature rise and/or temperature distribution based upon the known heat flux from the Thermal Actions.

In order to carry this out effectively the temperature field as a function of time has to consider:

— Heat transfer within the element (primarily by conduction for solid elements but also by convection and radiation when there are cavities/voids within the element),

— Migration of moisture and evaporation, degradation of the material

— Chemical reactions and phase changes which may be endothermic or exothermic

— Absorption of heat by adjacent materials

— Changes in physical characteristics.

Information required on the thermal properties will vary between materials but generally, they will include:

— Thermal conductivity

— Specific heat

— Density

— Emissivity

— Phase changes

— Moisture

— Charring rate.

It is important however, that attention is paid to how the properties were derived. Many test methods for determining material properties are carried out under steady-state conditions at elevated temperatures, whereas fire is a transient heating process. This is particularly important where there are physical and chemical changes, which would not be part of the laboratory test under a steady-state evaluation. Also of importance, is the rate of temperature rise in the material during the test, which must reflect the rate of temperature rise that the structural members may experience in the end use condition. However, some properties are relatively insensitive to whether they have been determined under steady-state or transient heating, or, even the rate of temperature rise.

The inputs into the heat transfer analysis can be a sub model in itself of how the properties vary during fire exposure. These are well documented in the Structural Eurocodes (EC's 2 to 6, and 9) for each of the materials used in load bearing construction.

In calculating the temperature field of structural elements various assumptions/simplifications can be made:

— **Uniform Temperature Cross Section:** Members that are totally engulfed in fire in which the structural elements are primarily made of materials with a high thermal conductivity (e.g. steel and aluminium alloys). However, sections with substantially different thicknesses in the web and flange e.g. deep plate girders, would be best treated as single elements within the section.

— **One Dimensional Heat Transfer:** Simple flat elements heated on one side (e.g. flat concrete floorslab) or axis-symmetric elements fully engulfed in fire (e.g. circular concrete or concrete filled column).

— **Two Dimensional Heat Transfer:** Analysis for determining the temperature field through the cross-section.

— **Three Dimensional Heat Transfer:** Analysis for determining the temperature field through its cross section and along its length.

5.1 Uniform temperature

5.1.1 Unprotected members

For uniform temperature distribution through the cross-section, the increase of temperature $\Delta\theta_{a,t}$ in an unprotected member during a time interval Δt, may be determined from:

$$\Delta\theta_{a,t} = \frac{A_\mathrm{m}/V}{c_\mathrm{a}\rho_\mathrm{a}} \dot{h}_{\mathrm{net,d}}\Delta t \qquad [0\,°\mathrm{C}] \tag{5.1}$$
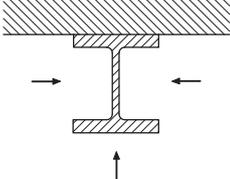
where:

A_m/V	is the section factor for unprotected members (see Table 4)	[m^{-1}]
A_m	is the exposed surface area of the member per unit length	[m^2]
V	is the volume of the member per unit length	[m^3]
c_a	is the specific heat of material used	[J/kgK]
$\dot{h}_{\mathrm{net,d}}$	is the design value of the net heat flux per unit area	[W/m^2]
Δt	is the time interval	[s]
ρ_a	is the unit mass of material	[kg/m^3]

The value of Δt, which is related to the section factor and shape of the thermal action, should generally, not be greater than 5 seconds, although depending upon the method adopted such as with a backward difference scheme, the time increments can be extended without loosing any accuracy.

In the above equation, the value of the section factor, A_m/V should not be used if it is less than 10 m^{-1}.

In Eurocode 3 on Fire Actions, a view (shadow) factor) is introduced where for example the entire cross section does not fully see the radiation from the fire.

In [Figure 8](#) it is recognized that for several exposure conditions, the member is not entirely exposed. The portion of the element where this occurs could be analysed more accurately by considering one dimensional heat flow towards the insulator.

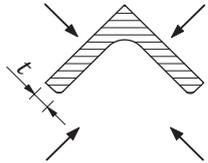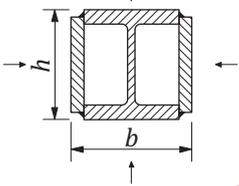| Open section exposed to fire on all sides:	Tube exposed to fire on all sides:
$\dfrac{A_m}{V} = \dfrac{\text{perimeter}}{\text{cross - section area}}$	$A_m/V = 1/t$
Open section exposed to fire on three sides:	Hollow section (or welded box section of uniform thickness) exposed to fire on all sides:
$\dfrac{A_m}{V} = \dfrac{\text{surface exposed to fire}}{\text{cross - section area}}$	If $t \ll b$: $A_m/V \approx 1/t$
I-section flange exposed to fire on three sides:	Welded box section exposed to fire on all sides:
$A_m/V = (b + 2t_f)/(bt_f)$ If $t \ll b$: $A_m/V \approx 1/t_f$	$\dfrac{A_m}{V} = \dfrac{2(b+h)}{\text{cross - section area}}$
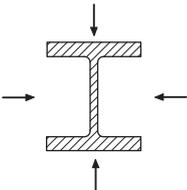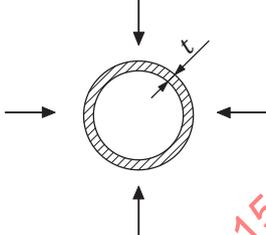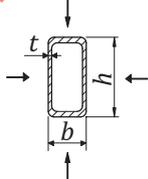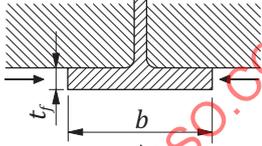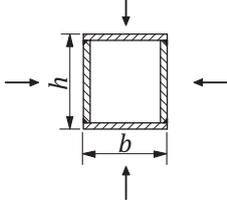
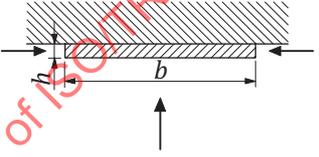| Angle (or any open section of uniform thickness) exposed to fire on all sides:	I-section with box reinforcement, exposed to fire on all sides:
$A_m/V = 2 / t$	$$\dfrac{A_m}{V} = \dfrac{2(b + h)}{\text{cross - section area}}$$
Flat bar exposed to fire on all sides:	Flat bar exposed to fire on three sides:
$A_m/V = 2(b + t) / (bt)$ If $t \ll b$: $A_m/V \approx 2 / t$	$A_m/V = (b + 2t) / (bt)$ If $t \ll b$: $A_m/V \approx 1 / t$
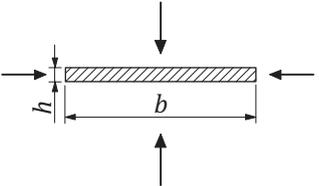
Figure 8 — Section factor, A_m/V for unprotected structural steel members

5.1.2 Protected members

5.1.2.1 Passive protection – boards and sprays

For a uniform temperature distribution in a cross-section, the temperature increase $\Delta\theta_{a,t}$ of an insulated member during a time interval Δt may be obtained using the following relationship:

$$\Delta\theta_{a,t} = \frac{\lambda_p A_p / V}{d_p c_a \rho_a} \frac{(\theta_{g,t} - \theta_{a,t})}{(1+\varphi/3)} \Delta t - (e^{\phi/10} - 1)\Delta\theta_{g,t} \qquad [^{\circ}C] \qquad (5.2)$$

But:

$$\Delta\theta_{a,t} \geq 0$$

With:

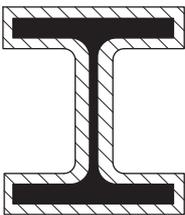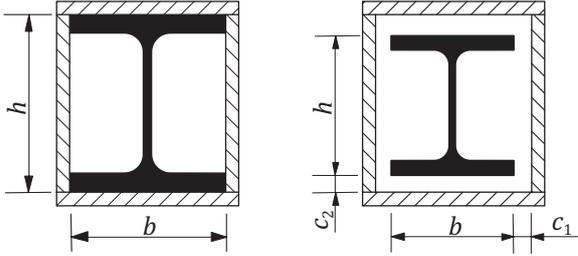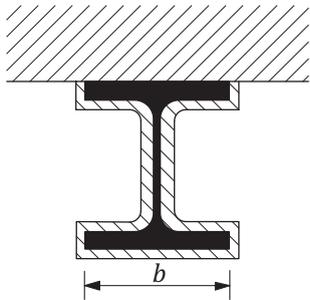$$\phi = \frac{c_p \rho_p}{c_a \rho_a} d_p A_p / V \qquad [^{\circ}C] \qquad (5.3)$$
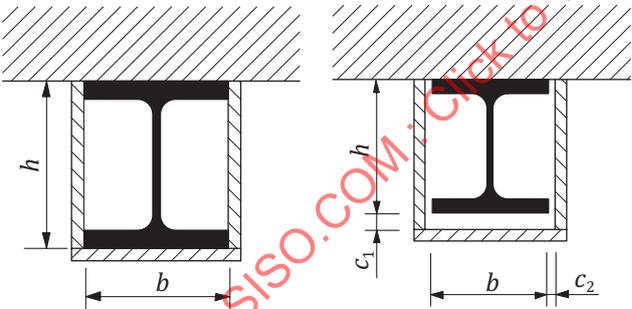
Where:

A_p/V	is the section factor for members insulated by fire protection material	[m^{-1}]
A_p	is the appropriate area of fire protection material per unit length of the member	[m^2/m]
V	is the volume of the member per unit length	[m^3/m]
c_a	is the specific heat of the steel element	[J/kgK]
c_p	is the specific heat of the fire protection material	[J/kgK]
d_p	is the thickness of the fire protection material	[m]
Δt	is the time interval	[s]
$\theta_{a,t}$	is the steel temperature at time t	[°C]
$\theta_{g,t}$	is the ambient gas temperature at time t	[°C]
$\Delta\theta_{g,t}$	is the increase of the ambient gas temperature during the time interval Δt	[°C]
λ_p	is the thermal conductivity of the fire protection material	[W/mK]
ρ_a	is the density of steel	[kg/m^3]
ρ_p	is the density of the fire protection material	[kg/m^3]

The values of c_p, ρ_p and λ_p (versus temperature) can be determined as individual values using standard laboratory techniques following specific test standards. They can also be determined based upon furnace tests and assessment methods such as ISO 834-10, ISO 834-11 or EN 13381. However, care should be taken when applying the thermal properties based upon furnace tests to other fire severities.

The time interval Δt, should not be greater than 30 s.

The area A_p, of spray fire protection material is generally taken as the area of its inner surface. For board fire protection, (hollow encasement) with a clearance around the member, the same value as for hollow encasement without a clearance may be adopted.

The section factors for steel elements protected with boards and sprays are illustrated in Figure 9.

Sketch	Description	Section factor (A_p/V)
	Contour encasement of uniform thickness	$\dfrac{\text{Metal perimeter}}{\text{Metal cross-section area}}$
	Hollow encasement[a] of uniform thickness	$\dfrac{2\,(b+h)}{\text{metal cross-section area}}$
	Contour encasement of uniform thickness, exposed to fire on three sides	$\dfrac{\text{Metal perimeter} - b}{\text{Metal cross-section area}}$
	Hollow encasement[a] of uniform thickness, exposed to fire on three sides	$\dfrac{2h+b}{\text{metal cross-section area}}$
[a] The clearance dimensions c_1 and c_2 should not normally exceed $h/4$.		

Figure 9 — Section factor A_p/V for steel members insulated by passive fire protection material

For most fire protection materials, the calculation of the element temperature increase $\Delta\theta_a$, may be modified to allow for a time delay in the rise of the element temperature when it reaches 100 °C. The duration of the plateau, at this temperature level has to be in relation with the amount of water in the protection material. See 5.2.2.

5.1.2.2 Reactive – intumescent coatings

Intumescent coatings or reactive coatings expand upon heating and provide an insulating char to protect structural steelwork. This char reduces the heat transfer to structural steel sections and therefore the steel follows a significantly reduced rate of temperature rise when compared with the fire temperature.

The thermal insulating performance of intumescent coatings are dependent on their chemical composition and thickness (dry-film thickness) with the latter determined as a function of the section factor. Each of these dependencies will be explained in the following.

Intumescent coatings have a basic make up in their formulation:

— A material that is able to foam up or expand to form typically a carbonaceous char.

— A material that under the action of heat releases an acid.

— A material that reacts with the acid (blowing agent) that releases gas (typically CO_2).

The thickness of char may be between 5 to 60 mm thick and because the material is very friable some systems include a fibre reinforcement to provide additional resistance to the turbulent flow and erosion forces of the hot gases.

The intumescing action is highly temperature dependent and the chemical composition of the coatings is chosen in such a way that the coating is most effective in the temperature range of interest. For structural steel this is typically 500 °C – 600 °C.

By applying greater coating thicknesses to steel members increases the thickness of the insulating char and hence the insulating performance. However, for thin film coatings in particular, there is a limited on the thickness of coating that can be applied in any one sequence of application, which can influence their commercial competitiveness. Typically coating thicknesses up to 1.0mm can be applied in a single coat. From experiments it is known that the fire resistance time of structural steelwork, i.e. the performance time in minutes to keep the steel below a certain critical temperature level, increases with increasing dry film thickness. However, the ratio of the intumesced char with respect to the original coating thickness does not remain the same as the thickness of the applied coating is increased. For very thick coatings, the efficiency of the charring action (foaming) is reduced and the insulating char prevents the non-reactive underlying layers becoming fully involved i.e. the insulating char starts to insulate itself.

The section factor has an influence on the behaviour of intumescent coatings. The lower the section factor the greater the heat sink and therefore better performance times are achieved for steel sections with low section factors than with high section factors for identical thicknesses.

In the early stages of the heating, there is a massive temperature gradient through the dry film and this would be influenced by the massivity of the protected members. As a result other physical phenomena may also take place that can affect the overall insulating performance of the coating. For example, the coating may flake or the foaming action may not be as efficient when compared with a thin coating. It is generally known that intumescent coatings perform more efficiently when exposed to high rates of temperature rise.

Modelling of the performance of reactive coatings is complicated because the thickness of the protection layer changes continuously over time and temperature. Moreover the chemical composition of the insulating char changes as function of time and temperature, causing specific heat, thermal conductivity and density to change continuously during the heating process. Therefore in order to quantify the heat transfer characteristics through the reactive coating to the steel section and establish the relationship between coating thickness, section factor, duration of fire resistance, a methodology as presented in ISO 834-11 is used.

The heat transfer is calculated as function of time using the following equation

$$\Delta\theta_a = \frac{K_{eff}}{\rho_a \, c_a \cdot} \cdot A_m / V \, (\theta_f - \theta_a) \cdot \Delta t \qquad [°C] \tag{5.4}$$

where:

$\Delta\theta_a$	is the temperature rise of the steel section in time step Δt	[°C]
K_{eff}	is the effective heat transfer coefficient	[W/m^2 °C]
ρ	is the density of steel	[7850 kg/m^3]
c_a	is the specific heat of steel, temperature dependent	[J/kg °C]
A_m/V	is the section factor of the steel section	[m^{-1}]
θ_f	is the furnace temperature at time t	[°C]
θ_a	is the average steel temperature at time t	[°C]
Δt	is a time step	[s]

The effective heat transfer coefficient is a function of dry film thickness, temperature and section factor and can be determined by linear regression in which an effective value for thermal conductivity K_{eff} is determined from the following equation:

$$K_{eff} = \frac{1}{dft}\left(C_0 + C_1 \cdot dft + C_2 \cdot \theta + C_3 A_m / V \right) \qquad [W/m^2{}°C] \tag{5.5}$$

where:

dft   is the dry film thickness [m]

C_0, C_1, C_2 and C_3 are dimensionless constants

Once the thermal conductivity is determined the effective insulation K_{eff} can be derived for various thicknesses of intumescent coating.

Internal sections protected by membranes

The fire resistance performance of a floor construction can be enhanced by the ceiling underneath providing it remains in place. The ceiling acts as a protective membrane and shields the floor construction from direct exposure from the fire. The temperature in the void follows a reduced fire temperature. Heat transfer is by radiation form the unexposed face and convection from the rising air currents. The performance of the ceiling construction itself, i.e. opening up of gaps, distortion of the grid, falling out of tiles, deformation of the ceiling, is influenced by the floor construction above. If the chosen floor provides a high resistance against heat transfer the temperature in the void will be higher. This has a negative effect on the performance of the ceiling construction. High cavity temperatures cause a more onerous effect on the ceiling construction with respect to opening up of gaps and distortion of the supporting lightweight structure and this can lead to ceiling tiles falling out prematurely.

Aerated concrete floor slabs (600 kg/m^3) have higher resistance to heat transfer than a normal dense concrete floor (2 400 kg/m^3). For this reason the temperature in a cavity under an aerated concrete floor will generally be higher than under a normal concrete floor.

In contrast, a timber floor has better insulation characteristics than an aerated concrete floor. Therefore the cavity temperature under a timber floor will generally be higher than that under an aerated concrete floor and will certainly be higher than under a normal concrete floor.

Furthermore, the air tightness of the floor construction has a great influence on the fire performance of the ceiling. The ceiling provides a better contribution to the fire resistance of the floor construction when the system is gas/air tight thus preventing hot gases penetrating into the void.

For a very simple conservative (safe) approximation of the temperature rise of steel members contained within the cavity, the ceiling membrane can be treated as three sided box protection system. This ignores the influence of the void and that the fact that the steel member only sees part of the radiating surfaces from the unexposed face of the ceiling.

5.2   Non uniform heating

5.2.1   General

Transient heat conduction problems involve the change in the energy content of a medium with time. The medium is divided into volume elements and the heat transferred into the volume element from all of its surfaces is calculated for each time-step Δt.

Noting that:

$$\Delta E_{element} = m \cdot C \cdot \Delta t = P \cdot V_{element} C \cdot \frac{T_m^{i+1} - T_m^i}{\Delta t} \tag{5.6}$$

where:

T_m^i and T_m^{i+1} are the temperatures of node m at times $t_i = i \Delta t$ and $t_{i+1} = (i + 1) \Delta t$, respectively

$T_m^{i+1} - T_m^i$ represents the temperature change of the node during the time interval Δt between the time steps i and i + 1.

The nodal temperatures in transient problems normally change during each time step. It is therefore possible to use temperatures at the previous time step i or the new time step $i + 1$ for the terms on the left side of the above equation. Both approaches are used in practice.

The finite element approaches are referred to as the **explicit method** (used the most) or the **implicit method** and are expressed in the general form as follows:

$$\sum_{allsides} Q^i + G_{element}^i = p \cdot V_{element} \cdot C - \frac{T_m^{i=1} + T_m^i}{\Delta t} \tag{5.7}$$

(Note: unstable if large time steps are used)

Implicit method:

$$\sum_{allsides} Q^{i+1} + G_{element}^{i+1} = p \cdot V_{element} \cdot C \frac{T_m^{i+1} - T_m^i}{\Delta t} \tag{5.8}$$

Both formulations are simply expressions between the nodal temperatures before and after a time interval and are based on determining the new temperatures T_m^{i+1} using the previous temperatures T_m^i.

The explicit method is easy to implement but imposes a limit on the allowable time step to avoid instabilities in the solution.

5.2.2   Migration of moisture

The moisture content of several of the structural materials has an important effect in the transfer of heat throughout the system.

Moisture can exist either in the form of free water, which is present in materials such as concrete (~2-3 % in a dry building) or timber (~10 % in a dry building) as well as chemically combined water. During heating, energy is absorbed as the water turns into a vapour (latent heat due to vaporization), or is freed in the course of a chemical reaction.

The change in the energy content of the volume element during Δt, is expressed as follows:

$$\Delta E_{element} = m \cdot c \cdot \Delta t \qquad (5.9)$$

or

$$\Delta E_{element} = p \cdot v_{element} \cdot c \cdot \Delta t \qquad (5.10)$$

where:

  p is density [Kg/m³]

  c is the specific heat of the element [kJ/kg°C].

Dividing the relation above by Δt gives:

$$\sum_{allsides} \dot{Q} + G_{element} = \frac{\Delta E_{element}}{\Delta t} = p \cdot v_{element} \cdot c \cdot \frac{\Delta T}{\Delta t} \qquad (5.11)$$

Where moisture is present, the term $\dot{G}_{element}$, i.e. the heat generated within the volume element during Δt, has a negative sign. Heat is dissipated as the moisture evaporates.

The specific heat of water is given by C_w = 4.18 kJ/kg°C.

The latent heat of vaporization of water is 2 256 kJ/kg.

The specific heat of water C_w is used to calculate the temperature rise in the volume element from ambient up to 100 °C. At this temperature, a phase change takes place in which water turns to steam. This therefore removes thermal energy from the system (volume element).

The temperature in the volume element will remain at 100 °C as long as there is moisture present and this gives rise to a moisture plateau. Although in Eurocode 2 the water is assumed to evaporate between 100 and 200 °C.

The duration of the moisture plateau length can be calculated as follows:

Input data:

  p is the density of the material [kg/m³]

  m is the moisture content of the material [kg/kg]

  d is the thickness of the material [m]

1 m^2 of the material weighs:

$$d \times 10^{-3} \cdot p = w \qquad [\text{kg/m}^2]$$

(5.12)

1 m^2 contains water:

$$m \cdot w = v \qquad [\text{kg/m}^2]$$

(5.13)

Total energy content needed for evaporation:

$$V \cdot C_w = Q \qquad [\text{J/m}^2]$$

(5.14)

The heat transfer to the volume element can be calculated using (5.9) and is h W/m^2 = h. J/s.m^2

Every minute the energy content Q is decreased with h. J/s m^2;

Hence the length of the moisture plateau is given by:

$$L = \frac{Q}{h} \qquad [\text{s}]$$

(5.15)

5.2.3 One dimensional temperature distribution

The change in the energy content of the volume element of a node m during a time interval Δt can be expressed as:

$$p \cdot c \cdot v \cdot \Delta T = p \cdot v \cdot c \cdot \left(T_m^{i+1} - T_m^i \right) \qquad [\text{kg}^4\text{m}^{-3}\text{K}]$$

(5.16)

where:

ρ	is the density	[kg/m^3]
V	is the volume element	[m^3]
ρV	is the mass	[kg]
C	is the specific heat	[J/kgK]
ΔT	is the temperature change	[K]

$$\sum_{all\ sides} \dot{Q} + \dot{G}_{element} = \rho\ V_{element}\ C\ \frac{T_m^{i+1} - T_m^i}{\Delta t} \qquad [\text{J/s}]$$

(5.17)

where:

T_m^i and T_m^{i+1} are the temperatures of node m at times $t_i = i_1 \Delta t$ and $t_{i+1} = (i + 1) \Delta t$, respectively

$T_m^{i+1} - T_m^i$ represents the temperature change of the node during the time interval Δt between the time steps i and i + 1.

Transient one-dimensional heat conduction is considered in a plane wall of thickness L and constant conductivity k with a mesh size of Δx = L/M and nodes 0, 1, 2.., with M in the x-direction.

The volume element of a general interior node m involves heat conduction from two sides and the volume of the element is $V_{element} = A \, \Delta x$.

The transient finite difference formulation for an interior node can be expressed on the basis of Formula (5.16) as:

$$k \cdot A \frac{T_{m-1} - T_m}{\Delta x} + \frac{kA T_{m+1} - T_m}{\Delta x} + g_m \cdot A \cdot \Delta x = p \cdot A \cdot \Delta x \cdot c \frac{T_m^{i+1} - T_m^i}{\Delta t} \qquad [\text{J/s}] \qquad (5.18)$$

Formula (5.18) obtains the implicit finite difference formulation by expressing the left side at time step i + 1 (instead of i) as:

$$k \cdot A \frac{T_{m-1}^{i+1} - T_m^{1+1}}{\Delta x} + k \cdot A \frac{T_{m+1}^{i+1} - T_m^{i+1}}{\Delta x} + \dot{g}_m \cdot A \cdot \Delta x = p \cdot A \cdot \Delta x \cdot c \frac{T_m^{i+1} - T_m^i}{\Delta t} \qquad [\text{J/s}] \qquad (5.19)$$

5.2.4 Two dimensional temperature distribution

A rectangular region is considered in which heat conduction is significant in the x- and y- directions, and the depth is considered as the unit depth of $\Delta z = 1$ in the z- direction. The thermal conductivity k of the medium is assumed to be constant. Now the $x - y -$ plane of the region is divided into a rectangular mesh of nodal points spaced Δx and Δy apart in the $x -$ and $y -$ directions, respectively. A general interior node (m,n) is considered whose coordinates are $x = m\Delta x$ and $y = n\Delta y$.

The volume element centred about the general interior node (m,n) involves heat conduction from four sides (right, left, top and bottom) and the volume of the element is $V_{element} = \Delta x . \Delta y \times 1 = \Delta x . \Delta y$.

The transient finite difference formulation for a general interior node can be expressed on the basis of Formula (5.18) as:

$$k \cdot \Delta y \frac{T_{m-1,n} - T_{m,n}}{\Delta x} + k\Delta x \frac{T_{m,n+1} - Tm,n}{\Delta y} + k\Delta y \frac{T_{m+1,n} - T_{m,n}}{\Delta x} +$$

$$k \cdot \Delta x \frac{T_{m,n-1} - T_{m,n}}{\Delta y} = \rho \Delta x \Delta y C \frac{T_{m,n}^{i+1} - T_{m,n}^i}{\Delta t} \qquad [\text{J/s}] \qquad (5.20)$$

The explicit finite difference formulation is obtained by expressing the left side at time step *i*.

The implicit finite difference formulation is obtained by expressing the left side at time step *i* + 1.

5.2.5 Three dimensional temperature distribution

A cubic volume is considered in which heat conduction is significant in the $x -, y -$ and $z -$ directions.

The thermal conductivity k of the medium is assumed to be constant. Now the $x - y - z$ volume is divided into a rectangular mesh of nodal points spaced Δx, Δy and Δz apart in the $x, y -$ and $z -$ directions, respectively. A general interior node (m,n,p) is considered whose coordinates are $x = m\Delta x$ and $y = n\Delta y$ and $z = p\Delta z$.

The volume element centred about the general interior node (m,n,p) involves heat conduction from six sides (right, left, top, bottom, front and rear). The volume of the element is $V_{element} = \Delta x . \Delta y . \Delta z = \Delta x \Delta y \Delta z$. The transient finite difference formulation for a general interior node can be expressed as:

$$k \cdot \Delta y \cdot \Delta z \frac{T_{m-1,n,p} - T_{m,n,p}}{\Delta x} + k\Delta x \, \Delta z \frac{T_{m,n+1,p} - T_{m,n,p}}{\Delta y} +$$

$$k \cdot \Delta y \cdot \Delta z \frac{T_{m+1,n,p} - T_{m,n,p}}{\Delta x} + k \cdot \Delta x \cdot \Delta z \frac{T_{m,n-1,p} - T_{m,n,p}}{\Delta y} +$$

$$k \cdot \Delta x \cdot \Delta y \frac{T_{m,n,p-1} - T_{m,n,p}}{\Delta z} + k \cdot \Delta x \cdot \Delta y \frac{T_{m,n1,p+1} - T_{m,n,p}}{\Delta z}$$

$$= \rho \, \Delta x \, \Delta y \, \Delta z \, C \frac{T_{m,n,p}^{i+1} - T_{m,n,p}^{i}}{\Delta t} \qquad [\text{J/s}] \qquad\qquad (5.21)$$

The explicit finite difference formulation is obtained by expressing the left side at time step *i*.

The implicit finite difference formulation is obtained by expressing the left side at time step *I*+1.

5.3   Time equivalent

5.3.1   General

The 'time equivalent' technique is a method that is frequently used by engineers to quantify the exposure of a structural element in a 'real' fire to an equivalent period of heating by the same member in the 'Standard' furnace test.

The most well known formulations include

— Pettersson

— Harmathy

— Law

By Standard/Code:

— DIN 18230

— CIB W14

— Eurocode 1-1-2

Other:

— Graphical analysis.

The relationships described in DIN 18230, CIB W14 and Eurocode 1-1-2 are very similar in their approach with the main differences being in the treatment of the individual parameters.

There are limitations with respect to the application of time equivalent. For example, it is only applicable to post flashover fires, for unprotected steel correlation with fire resistance times in excess of 30 minutes is poor.

It should also be noted that some countries do not accept the concept of time equivalent and is limited to specific types of materials and construction systems.

5.3.2 Eurocode 1-1-2

The equation given in Eurocode 1-1-2 Annexe F is described by the following relationship:

$$t_{e,d} = q_{f,d} \times k_b \times w_f \qquad \text{[mins]}$$

(5.22)

where;

$q_{f,d}$ is the design fire load   [MJ/m^2]

k_b is an insulation factor for the compartment boundaries   [min·m^2/MJ]

w_f is a ventilation factor (dimensionless)   [-]

5.3.3 Graphical analysis

The graphical method is based upon correlating the maximum temperature attained by, for example, a protected steel member in a real fire, with an equivalent period of heating required to attain the same temperature in the Standard furnace test (ISO 834-1). This is illustrated schematically in Figure 10 for a protected steel member.
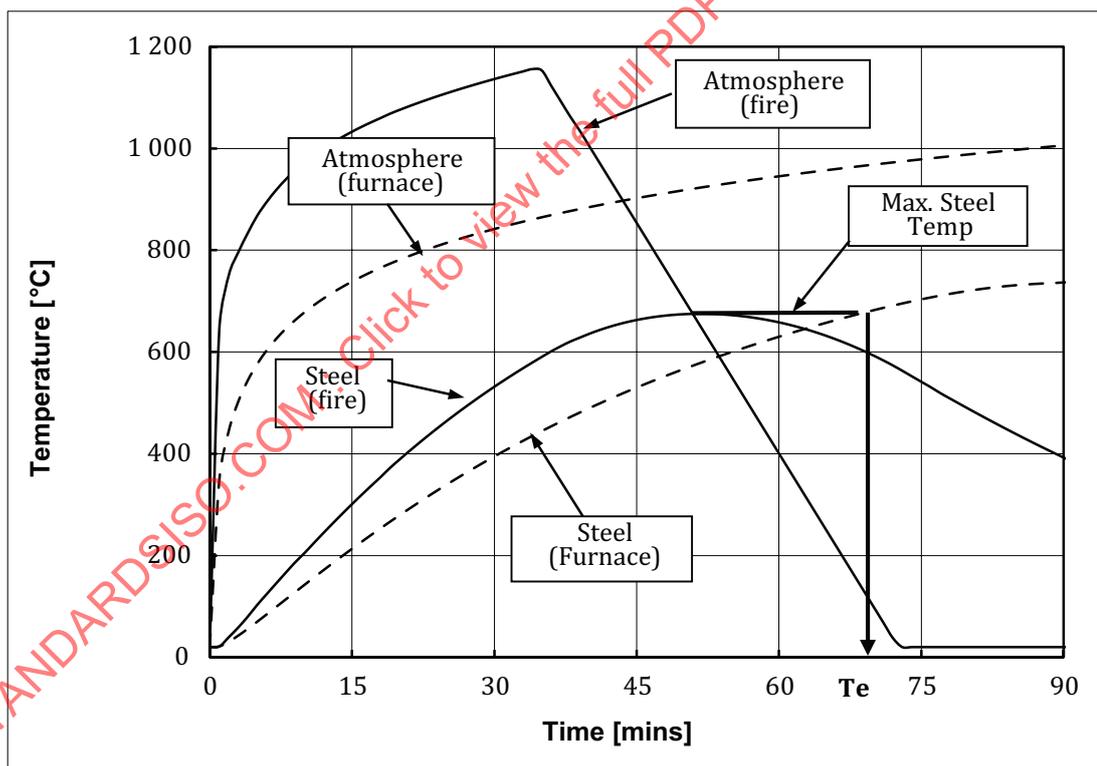

Figure 10 — Graphical method for time equivalent

5.3.4 Application of Monte Carlo analysis for determining time equivalent

The Monte Carlo technique is applicable to problems of a stochastic or probabilistic nature. It involves the simulation of a large sample of typical fire scenarios during which values for each design variable are chosen at random for input into engineering calculations. This makes up the probabilistic element of the methodology.

Probability distributions are required for each part of the model system. These can be derived from expert judgement, statistical data or real life observations and confidence in the results may be enhanced if the relationships built into the model are based upon accepted scientific theory supported by experimental data. Such simulation-based approaches are advantageous as they are based upon physical theory and experimental measurement and this can be used to compensate for a lack of information about real fires in a manner that other methods for calculating risk cannot. Furthermore, the assumptions made in these simulation models are explicit and a measure can be made of the sensitivity of these assumptions on the calculated risks by changing the values for each variable, recalculating the risk and comparing this new risk measure with that originally calculated. The sensitivity analysis can then be used to determine which variables have the greatest influence on the calculated risks and which variables are relatively unimportant.

The Monte Carlo method of analysis is ideally suited to practical applications since there is the opportunity to include a high level of detail and any shaped distribution can be used from which values can be chosen at random for use in engineering calculations. However, the values must be compatible with the known statistical distributions.

For example, in the UK Fire Safety Engineering Code, BS 7974, data are provided on the fire load densities for several occupancies at the 80 %, 90 %, 95 % fractile levels. Average values are also given. Therefore, if 100,000 values of fire load are selected they must conform to a statistical distribution fixed around the known datum points. In this particular example, a methodology was developed that enabled the full distribution of fire load densities to be described.

Other variables, such as room size, minimum and maximum window opening areas and room heights can be inputted into the model. These can be set to vary within a prescribed range or where there is statistical data they can be treated in a similar way to fire load density.

The Monte Carlo methodology for deriving time equivalent periods of fire exposure is illustrated in Figure 11 and is based upon the graphical method using protected steel members.

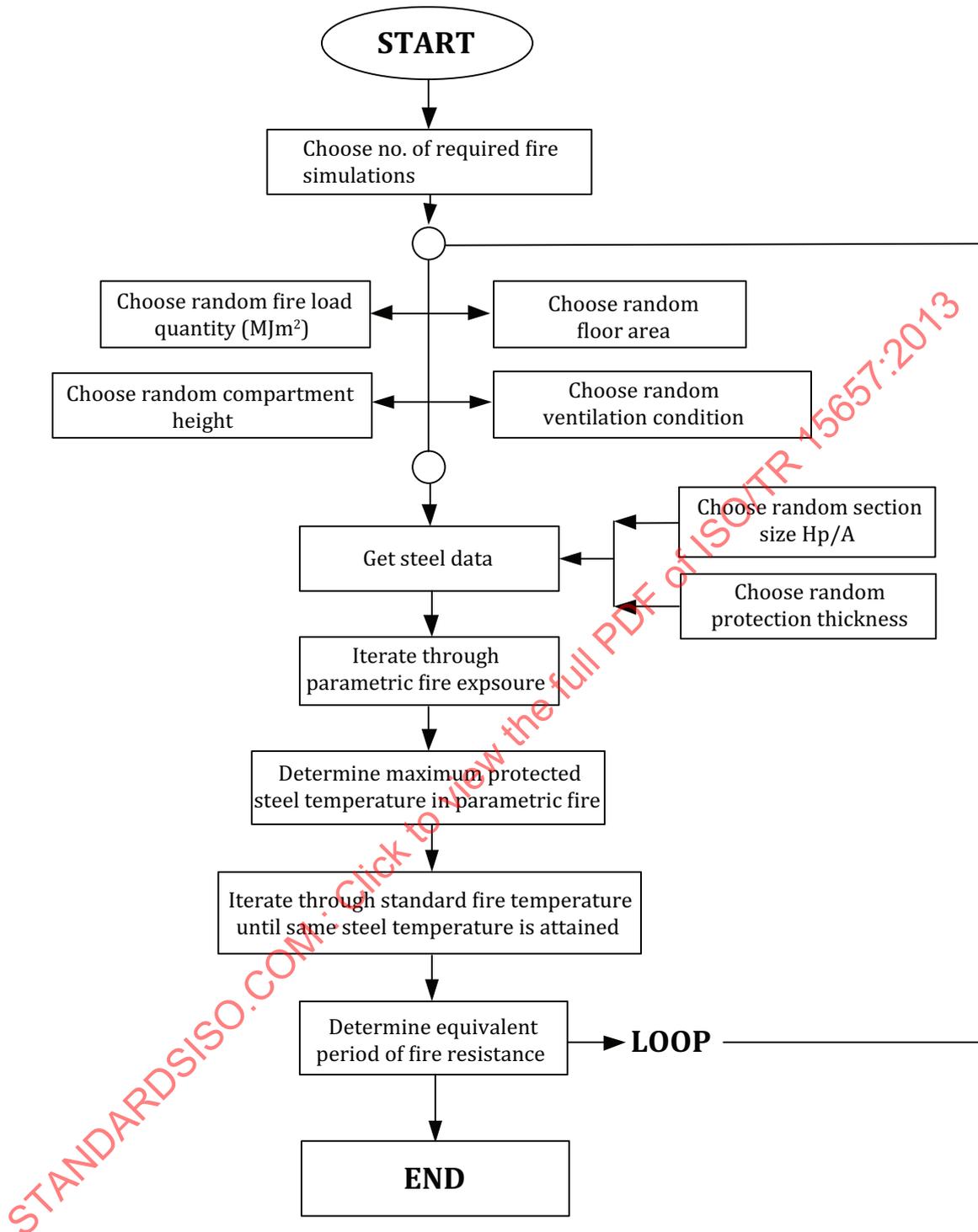**Figure 11 — Monte Carlo analytical technique**

Number of trials = 100,000

For I = 1 to Number of trials

— Select fire load

— Select compartment size

— Select ventilation

— Select compartment insulation properties

— Select section size

— Select fire protection thickness or thickness of cover to reinforcement

— Compute and store time equivalent

Next:

At the end of the process, 100,000 values of time equivalent are stored. It is convenient to plot these as percentage fractiles. For example, the 80 % fractile is the time equivalent value that is only exceeded in 20,000 of the 100,000 cases and the 90 % fractile corresponds to the value that is only exceeded in 10,000 of the 100,000 cases. A typical plot of cumulative % fractile value vs time equivalent fire resistance is illustrated in Figure 12, which also incorporates a separate curve with sprinkler fire protection taken into account.
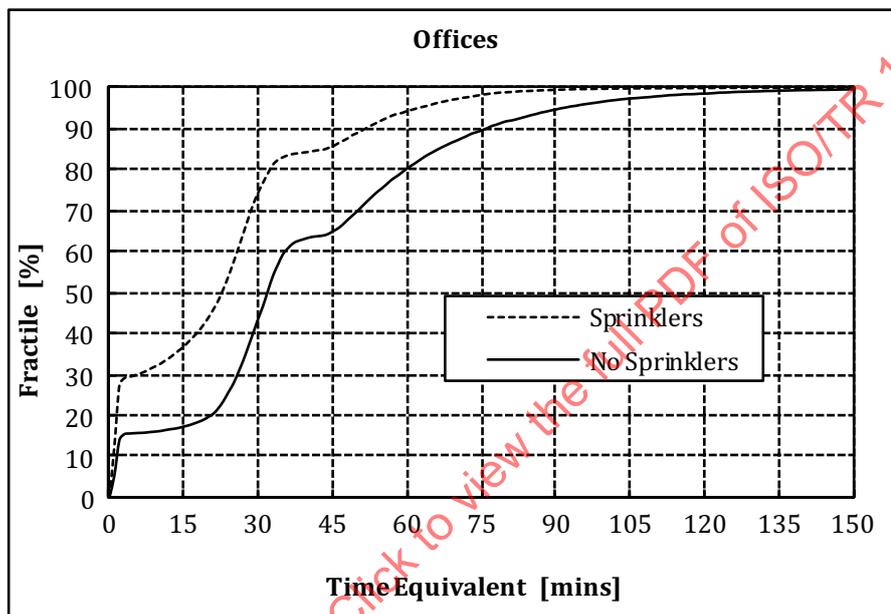
Offices

Figure 12 — Typical cumulative distribution output for Time Equivalent

6   Structural design

6.1   Mechanical properties

The following section describes the mechanical properties of materials that may be used to determine the mechanical behaviour of structural elements under standard furnace (nominal) heating conditions. In most cases the properties are also valid for structural elements exposed to real fires.

6.1.1   Concrete

6.1.1.1   Compressive strength

The strength and deformation properties of uniaxially stressed concrete at elevated temperatures can be described by two parameters in the Table 4 where:

$f_{c,\theta}$ is the compressive strength, and

$\varepsilon_{c1,\theta}$ is the strain corresponding to $f_{c,\theta}$

Values for $\varepsilon_{cu1,\theta}$ defining the range of the ascending branch are given in columns 4 and 7.

Table 4 — Values of the main parameters

Concrete Temp.	Siliceous Aggregates			Calcareous Aggregates		
°C	$f_{c,\theta}/f_{ck}$ [-]	$\varepsilon_{c1,\theta}$ [-]	$\varepsilon_{cu1,\theta}$ [-]	$f_{c,\theta}/f_{ck}$ [-]	$\varepsilon_{c1,\theta}$ [-]	$\varepsilon_{cu1,\theta}$ [-]
1	2	3	4	5	6	7
20	1.00	0.0025	0.0200	1.00	0.0025	0.0200
100	1.00	0.0040	0.00225	1.00	0.0040	0.0225
200	0.95	0.0055	0.0250	0.97	0.0055	0.0250
300	0.85	0.0070	0.0275	0.91	0.0070	0.0275
400	0.75	0.0100	0.0300	0.85	0.0100	0.0300
500	0.60	0.0150	0.0325	0.74	0.0150	0.0325
600	0.45	0.0250	0.0350	0.60	0.0250	0.0350
700	0.30	0.0250	0.0375	0.43	0.0250	0.0375
800	0.15	0.0250	0.0400	0.27	0.0250	0.0400
900	0.08	0.0250	0.0425	0.15	0.0250	0.0425
1000	0.04	0.0250	0.0450	0.06	0.0250	0.0450
1100	0.01	0.0250	0.0475	0.02	0.0250	0.0475
1200	0.00	-	-	0.00	-	-

Table 4 may be used for normal weight concrete with siliceous or calcareous (containing at least 80 % calcareous aggregate by weight) aggregates.

A mathematical model for stress strain relationships of concrete under compression at elevated temperatures may be described as given in Table 5.

Table 5 — Stress strain relationship for concrete at elevated temperatures

Range	Stress $\sigma(\theta)$
$\varepsilon \leq \varepsilon_{c1,\theta}$	$$\dfrac{3\varepsilon f_{c,\theta}}{\varepsilon_{c1,\theta}\left\{2+\left(\dfrac{\varepsilon}{\varepsilon_{c1,\theta}}\right)^3\right\}}$$
$\varepsilon_{c1(\theta)} < \varepsilon \leq \varepsilon_{cu1,\theta}$	For numerical purposes a descending branch should be adopted. Linear or non-linear models are permitted

The loss in compressive strength at elevated temperatures is illustrated in Figure 13.
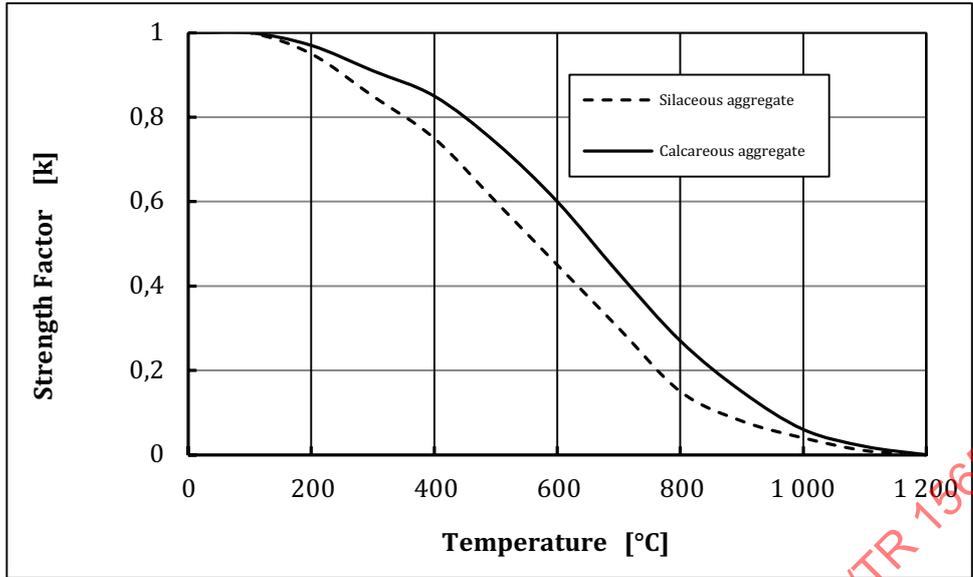
Figure 13 — Variation in compressive strength of concrete at elevated temperatures for siliceous and calcareous aggregates

6.1.1.2 Tensile strength

The tensile strength of concrete should normally be ignored (conservative). If it is necessary to take account of the tensile strength, when using the simplified or advanced calculation method the following may be used in which the reduction of the characteristic tensile strength of concrete is allowed for by the coefficient $k_{c,t}(\theta)$ as given in:

$$f_{ck,t}(\theta) = k_{c1t}(\theta) f_{ck,t} \qquad [\text{N/mm}^2]$$

(6.1)

In the absence of more accurate information the following $k_{c,t}(\theta)$ values should be used:

$$k_{c,t}(\theta) = 1.0 \text{ for } 20 \text{ °C} \leq \theta \leq 100 \text{ °C} \qquad [\text{-}]$$

(6.2)

$$k_{c,t}(\theta) = 1.0 - 1.0 \ (\theta - 100)/500 \text{ for } 100 \text{ °C} < \theta \leq 600 \text{ °C} \qquad [\text{-}]$$

(6.3)
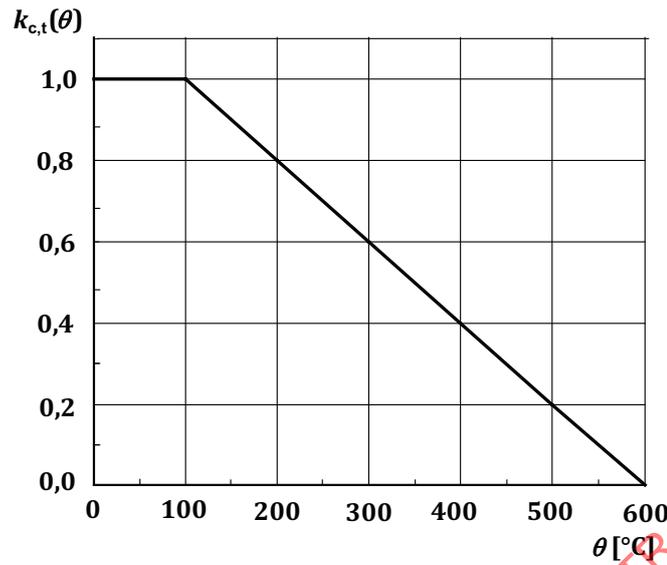
This is illustrated in Figure 14.

Figure 14 — Coefficient $kc_1t(\theta)$ alllowing for the decrease in tensile strength, fck,t, of concrete at elevated temperatures

6.1.2 Structural steel

6.1.2.1 Hot rolled carbon steel

6.1.2.1.1 Stress strain (transient state)

The stress strain relationship for structural steel is described by the relationships given in Table 6, which are also represented in Figure 5.

Table 6 — Stress strain relationship for structural steel

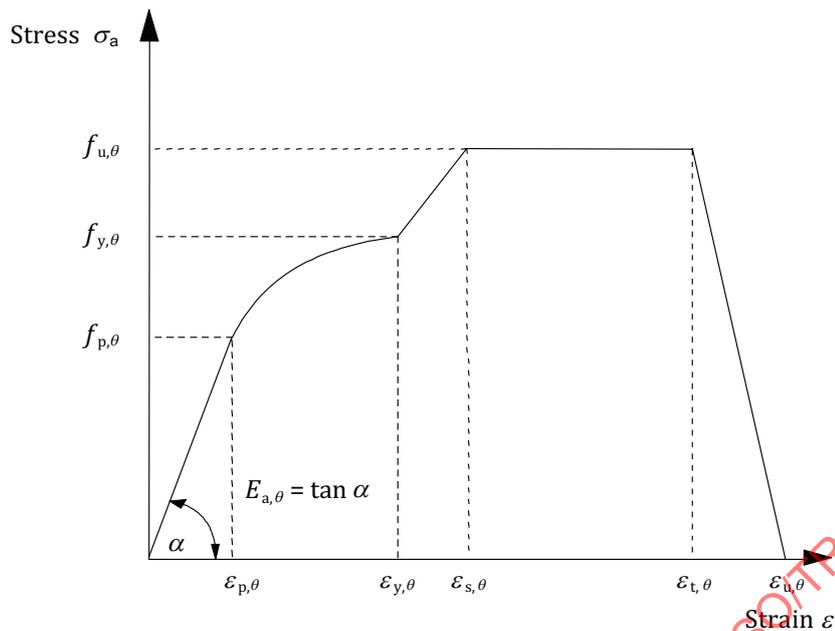| Strain range	Stress σ	Tangent modulus
$\varepsilon \le \varepsilon_{p,\theta}$	$\varepsilon E_{a,\theta}$	$E_{a,\theta}$
$\varepsilon_{p,\theta} < \varepsilon < \varepsilon_{y,\theta}$	$f_{p,\theta} - c + (b/a)[a^2 - (\varepsilon_{y,\theta} - \varepsilon)^2]^{0.5}$	$\dfrac{b\left(\varepsilon_{y,\theta} - \varepsilon\right)}{a\left[a^2 - \left(\varepsilon_{y,\theta} - \varepsilon\right)^2\right]^{0.5}}$
$\varepsilon_{y,\theta} \le \varepsilon \le \varepsilon_{t,\theta}$	$f_{y,\theta}$	0
$\varepsilon_{t,\theta} < \varepsilon < \varepsilon_{u,\theta}$	$f_{y,\theta}[1 - (\varepsilon - \varepsilon_{t,\theta})/(\varepsilon_{u,\theta} - \varepsilon_{t,\theta})$	-
$\varepsilon = \varepsilon_{u,\theta}$	0.00	-
Parameters	$\varepsilon_{p,\theta} = f_{p,\theta}$ $\varepsilon_{y,\theta} = 0.2$ $\varepsilon_{t,\theta} = 0.15$ $\varepsilon_{u,\theta} = 0.20$	
Functions	$a^2 = (\varepsilon_{y,\theta} - \varepsilon_{p,\theta})\ (\varepsilon_{y,\theta} - \varepsilon_{p,\theta} + c/E_{a,\theta})$ $b^2 = (\varepsilon_{y,\theta} - \varepsilon_{p,\theta})E_{a,\theta}\ `` + c^2$ $c = \dfrac{\left(f_{y,\theta} - f_{p,\theta}\right)^2}{\left(\varepsilon_{y,\theta} - \varepsilon_{p,\theta}\right)E_{a,\theta} - 2\left(f_{y,\theta} - f_{y,\theta}\right)}$	

Figure 15 — Schematic representation of the stress strain relationship for structural steel at elevated temperatures

where:

$f_{y,\theta}$ is the effective yield strength

$f_{p,\theta}$ is the proportional limit

$E_{a,\theta}$ is the slope of the linear elastic range

$\varepsilon_{p,\theta}$ is the strain at the proprtional limit

$\varepsilon_{y,\theta}$ is the yield strain

$\varepsilon_{t,\theta}$ is the limiting strain for yield strength

$\varepsilon_{u,\theta}$ is the ultimate strain

In addition, for temperatures up to 400 °C and strains greater than 2 %, an additional strain hardening component can be introduced. This data was not derived from transient tests and is described as:

2 % < $\varepsilon_{a\theta}$ < 4 %

4 % ≤ $\varepsilon_{a,\theta}$ ≤ 15 %

15 % < $\varepsilon_{a,\theta}$ < 20 %

$\varepsilon_{a,\theta}$ ≤ 20 %

The reduction factors for each property with strain hardening taken into account are given in Table 7.

The effect of strain hardening should only be considered if the analysis is based upon advanced calculation models and if it is shown that local failures i.e. local buckling, shear failure etc. do not occur due to increased strains.

Table 7 — Reduction factors, k_θ, for stress strain relationships of structural steel at elevated temperatures

Steel Temperature θ_a [°C]	$k_{E,\theta} = \dfrac{\overline{E}_{a,\theta}}{E_{a,20^0 C}}$	$k_{p,\theta} = \dfrac{f_{ap,\theta}}{f_{ay,20^0 C}}$	$k_{\max,\theta} = \dfrac{f_{a\max,\theta}}{f_{ay,20^0 C}}$	$k_{u,\theta} = \dfrac{f_{au,\theta}}{f_{ay,20^0 C}}$
0	1,00	1,00	1,00	1,25
100	1,00	1,00	1,00	1,25
200	0,90	0,807	1,00	1,25
300	0,80	0,613	1,00	1,25
400	0,70	0,42	1,00	
500	0,60	0,36	0,78	
600	0,31	0,18	0,47	
700	0,13	0,075	0,23	
800	0,09	0,05	0,11	
900	0,0675	0,0375	0,06	
1000	0,045	0,025	0,04	
1100	0,0225	0,0125	0,02	
1200	0,00	0,00	0,00	

The variation of these parameters with temperature are also illustrated in Figure 16.
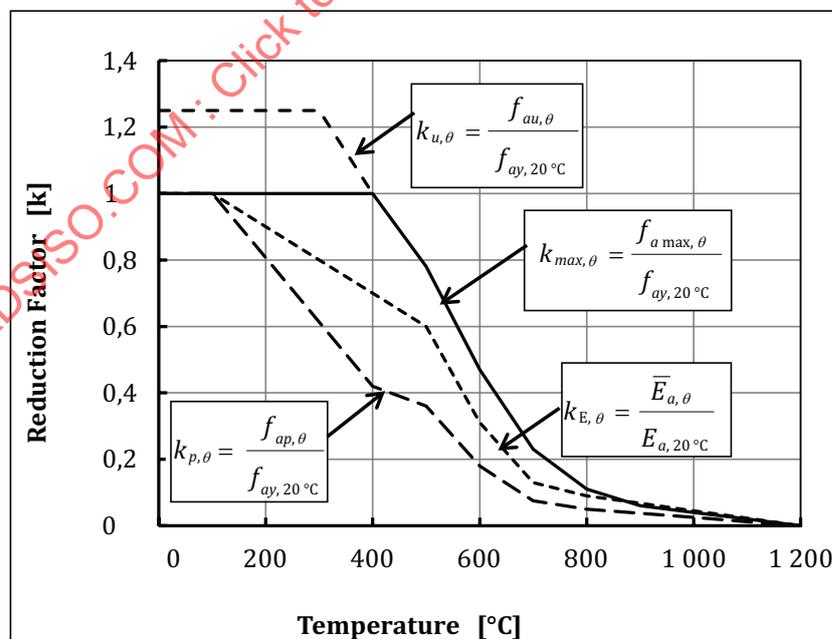

Figure 16 — Graphical representation of the factors, k_θ, given in Table 7

6.1.2.2 Hot rolled reinforcing steels

The strength and deformation properties of reinforcing steels at elevated temperatures may be obtained from the same mathematical expressions as given for structural steel.

6.1.2.3 Cold worked reinforcing steels

6.1.2.3.1 Young's (elastic) modulus and stress strain behaviour

The three main parameters describing the stress-strain relationship for cold worked reinforcing steels are given in Table 8.

Table 8 — Values for the three main parameters ($E_{s,\theta}$; $f_{sp,\theta}$; $f_{s\,max,\theta}$) of the stress-strain relationships for cold worked reinforcing steel

Steel temperature θ_s [°C]	$\dfrac{E_{s,\theta}}{E_{s,20°C}}$	$\dfrac{f_{sp,\theta}}{f_{sy,20°C}}$	$\dfrac{f_{s\,max,\theta}}{f_{sy,20°C}}$
20	1,00	1,00	1,00
100	1,00	0,96	1,00
200	0,87	0,92	1,00
300	0,72	0,81	1,00
400	0,56	0,63	0,94
500	0,40	0,44	0,67
600	0,24	0,26	0,40
700	0,08	0,08	0,12
800	0,06	0,06	0,11
900	0,05	0,05	0,08
1000	0,03	0,03	0,05
1100	0,02	0,02	0,03
1200	0,00	0,00	0,00

For the decreasing branch of the stress strain relationship the values for hot finished structural steel may be adopted.

6.1.2.4 Prestressed wires

The strength deformation characteristics of prestressing steel is given in Table 9 for cold worked (cw) wires and strands and for quenched and tempered (q&t) bars.

For cold worked bars and strands there are two classes (A&B) denoted by the value given to the factor, β, and is varied according to National practice.

Table 9 — Elevated temperature stress strain relationships for cold worked wires and strands and quench and tempered bars

Steel Temp θ [°C]	$f_{yp,\theta}/(\beta f_{pk})$			$f_{pp,\theta}/(\beta f_{pk})$		$E_{p,\theta}/E_p$		$\varepsilon_{pt,\theta}$ [-]	$\varepsilon_{pu,\theta}$ [-]
	CW Class A	CW Class B	Q&T	CW	Q&T	CW	Q&T	CW, Q&T	CW, Q&T
1	2a	2b	3	4	5	6	7	8	9
20	1.00	1.00	1.00	1.00	1.00	1.00	1.00	0.050	0.100
100	1.00	0.99	0.98	0.68	0.77	0.98	0.76	0.050	0.100
200	0.87	0.87	0.92	0.51	0.62	0.95	0.61	0.050	0.100
300	0.70	0.72	0.86	0.32	0.58	0.88	0.52	0.055	0.105
400	0.50	0.46	0.69	0.13	0.52	0.81	0.41	0.060	0.110
500	0.30	0.22	0.26	0.07	0.14	0.54	0.20	0.065	0.115
600	0.14	0.10	0.21	0.05	0.11	0.41	0.15	0.070	0.120
700	0.06	0.08	0.15	0.03	0.09	0.10	0.10	0.075	0.125
800	0.04	0.05	0.09	0.02	0.06	0.07	0.06	0.080	0.130
900	0.02	0.03	0.04	0.01	0.03	0.03	0.03	0.085	0.135
1000	0.00	0.00	0.00	0.00	0.00	0.00	0.00	0.090	0.140
1100	0.00	0.00	0.00	0.00	0.00	0.00	0.00	0.095	0.145
1200	0.00	0.00	0.00	0.00	0.00	0.00	0.00	0.100	0.150

NOTE   For intermediate values of temperature, linear interpolation may be used.

6.1.2.5 Stainless steels

6.1.2.5.1 Strength characteristics, Young's (elastic) modulus and stress –strain behaviour

The stress strain behaviour of stainless steel is shown schematically in Figure 17 and for each grade can be described by the mathematical relationships given in Table 10.

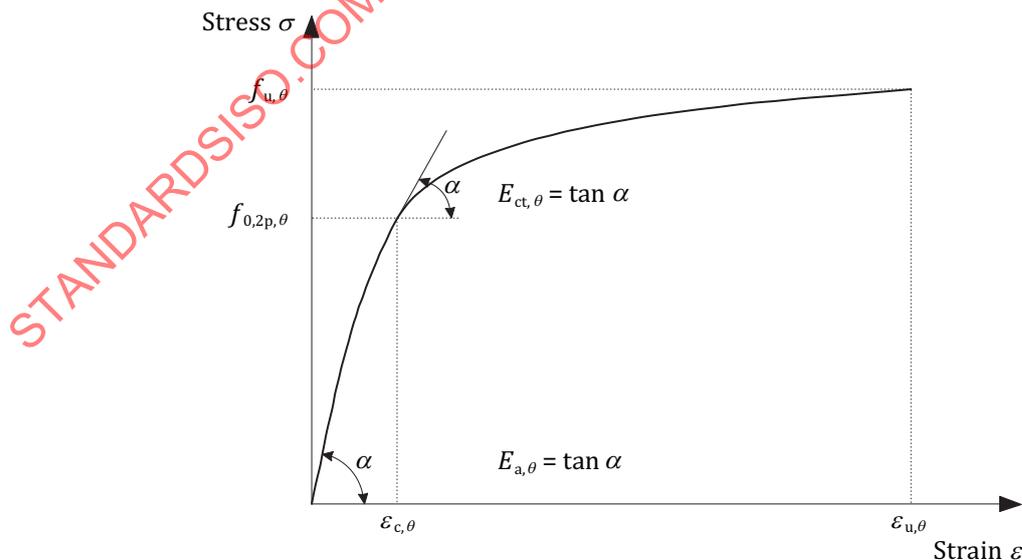**Figure 17 — Stress strain model for stainless steel at elevated temperature**

Table 10 — Stress strain parameters for stainless steel

Strain range ε	Stress σ	Tangent modulus E_t
$\varepsilon \le \varepsilon_c$	$\dfrac{E\varepsilon}{1+a\varepsilon^b}$	$\dfrac{E(1+a\varepsilon^b - ab\varepsilon^b)}{(1+a\varepsilon^b)}$
$\varepsilon_c \le \varepsilon \le \varepsilon_u$	$f_{0.2p} - e + \dfrac{d}{c}\sqrt{c^2 - (\varepsilon_u - \varepsilon)^2}$	$\dfrac{d + (\varepsilon_u - \varepsilon)}{c\sqrt{c^2 - (\varepsilon_u - \varepsilon)^2}}$

where:

$$a = \frac{\left(E\varepsilon_r - f_{0.2p}\right)}{f_{0.2p}\varepsilon_c^b} \qquad [\text{-}] \tag{6.4}$$

$$b = \frac{\left(E_{ct}\varepsilon_c / f_{0.2p}\right)}{\left(E\varepsilon_c / f_{0.2p} - 1\right)}\frac{E\varepsilon_c}{f_{0.2p}} \qquad [\text{-}] \tag{6.5}$$

$$C^2 = \left(\varepsilon_u - \varepsilon_c\right)\left(\varepsilon_u - \varepsilon_c + \frac{e}{E_{ct}}\right) \qquad [\text{-}] \tag{6.6}$$

$$d^2 = e\left(\varepsilon_u - \varepsilon_c\right)E_{ct} + e^2 \qquad [\text{-}] \tag{6.7}$$

$$e = \frac{\left(f_u - f_{0.2p}\right)^2}{\left(\varepsilon_u - \varepsilon_c\right)E_{ct} - 2\left(f_u - f_{0.2p}\right)} \qquad [\text{-}] \tag{6.8}$$

with $\varepsilon_c = f_{0.2p}/E + 0.002$ and $f_{0.2p}$ the 0.2 % proof stress of stainless steel.

For structural design in fire, three sets of parameters are necessary to describe the behaviour at elevated temperatures. These are:

Elastic modulus:

$$k_{E\theta} = \frac{E(\theta)}{E(20\,°\text{C})} \qquad [\text{-}] \tag{6.9}$$

0.2 % proof strength:

$$k_{0.2p,\theta} = \frac{f_{0.2p}(\theta)}{f_{0.2p}(20\,°\text{C})} \qquad [\text{-}] \tag{6.10}$$

2 % absolute strain strength = $k_{2\%\theta}$

Ultimate tensile strength:

$$k_{u,\theta} = \frac{f_u(\theta)}{f_u(20\,°\text{C})} \qquad [\text{-}] \tag{6.11}$$

The parameters are given for example in Table 11.

Table 11 — Various parameters for stress strain relationships at elevated temperatures for stainless steel grade EN 14462

Temp. (°C)	$\dfrac{E(\theta)}{E(20\,°C)}$	$\dfrac{f_{0.2p}(\theta)}{f_{0.2p}(20\,°C)}$	$\dfrac{E_{ct}(\theta)}{E(20\,°C)}$	$\dfrac{f_u(\theta)}{f_u(20\,°C)}$	ε_u	$k_{2\%\theta}$
20	1.00	1.00	0.100	1.00	0.20	0.35
100	0.96	0.91	0.070	0.93	0.20	0.35
200	0.92	0.80	0.037	0.85	0.20	0.32
300	0.88	0.75	0.035	0.83	0.20	0.30
400	0.84	0.72	0.033	0.82	0.20	0.28
500	0.80	0.65	0.030	0.71	0.20	0.30
600	0.76	0.56	0.030	0.57	0.20	0.33
700	0.71	0.37	0.025	0.38	0.15	0.40
800	0.63	0.26	0.025	0.29	0.15	0.41
900	0.45	0.10	0.025	0.12	0.15	0.45
1000	0.20	0.03	0.025	0.04	0.15	0.47

6.1.3 Timber

On exposure to fire, the outermost surface of timber elements burns, forming a char. Continued exposure results in a gradual erosion of the surface and the extension of the charred zone further into the depth of the timber. It may be assumed that only charred timber is affected by fire and the internal residual uncharred section will be capable of maintaining a loadbearing function. The timber element will continue to carry its design load only as long as the unaffected residual section retains a sufficient load carrying capacity.

6.1.3.1 Strength in Compression, Tension and Shear

The strength for softwoods at elevated temperatures can be determined by multiplying the temperature reduction factor according to Figure 18.
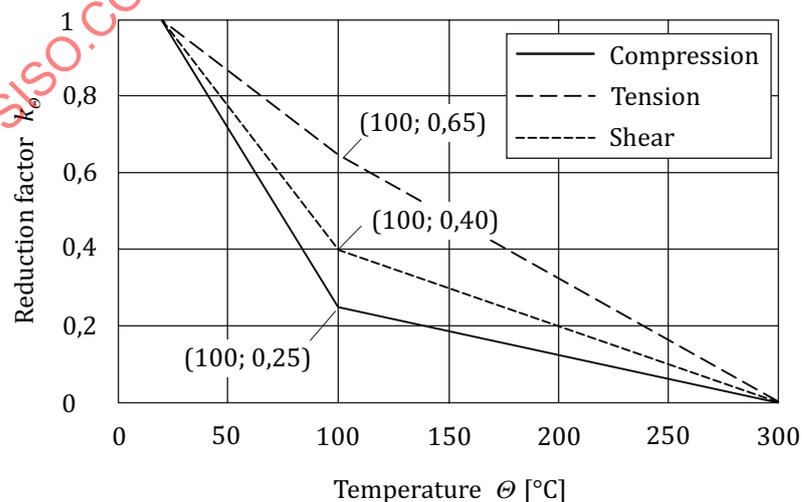
Figure 18 — Reduction factor for strength parallel to the grain for softwood

6.1.3.2 Elastic modulus in tension and compression

The elastic modulus for softwoods at elevated temperatures can be determined by multiplying the temperature reduction factor according to Figure 19.
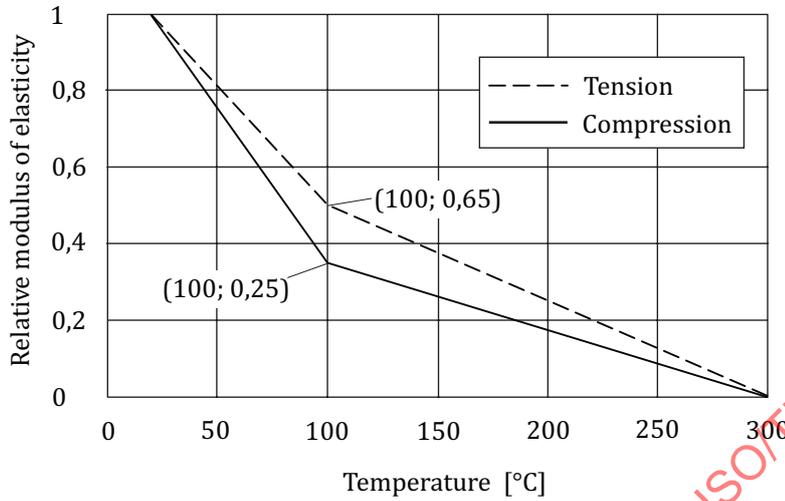

Figure 19 — Effect of temperature on the elastic modulus of softwood parrallel to the grain

For compression perpendicular to the grain the same reduction of strength may be applied as for compression parallel to the grain.

For shear with both stress components perpendicular to the grain (rolling shear), the same reduction of strength may be applied as for compression parallel to the grain.

6.1.4 Masonry

6.1.4.1 Stress strain behaviour

The temperature dependent stress strain behaviour of masonry units is a function of the material, strength and density. Examples of several common types are given in Figures 20 to 22.
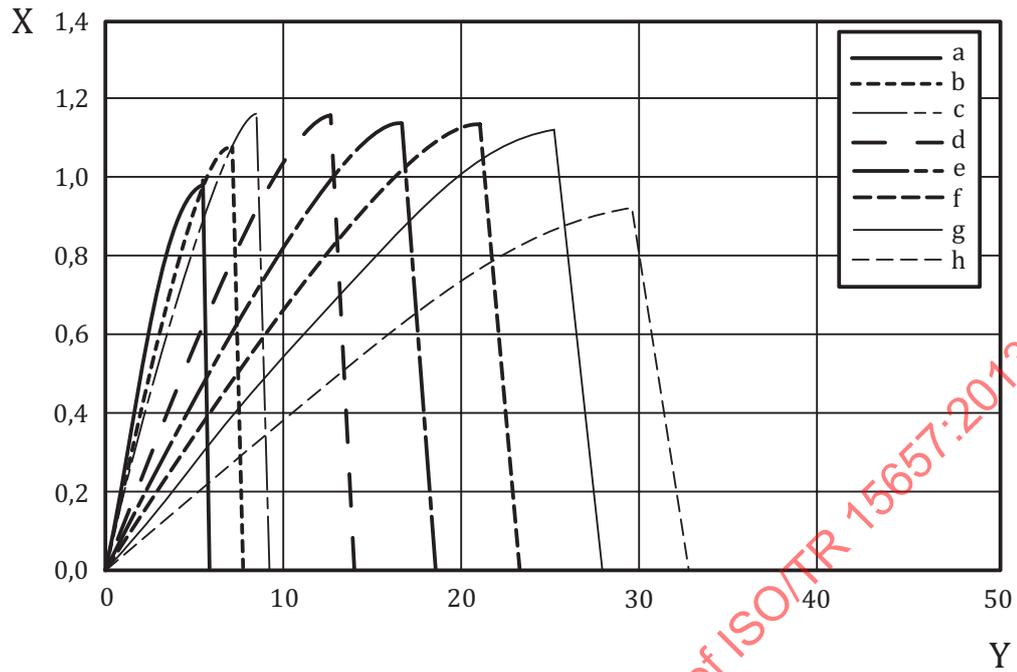
Figure 20 — Temperature dependent stress strain diagrams for lightweight aggregate concrete units(pumic) with unit strength of 4 – 6 N/mm² and with a denisty range of 600 – 1 000 kg/m³
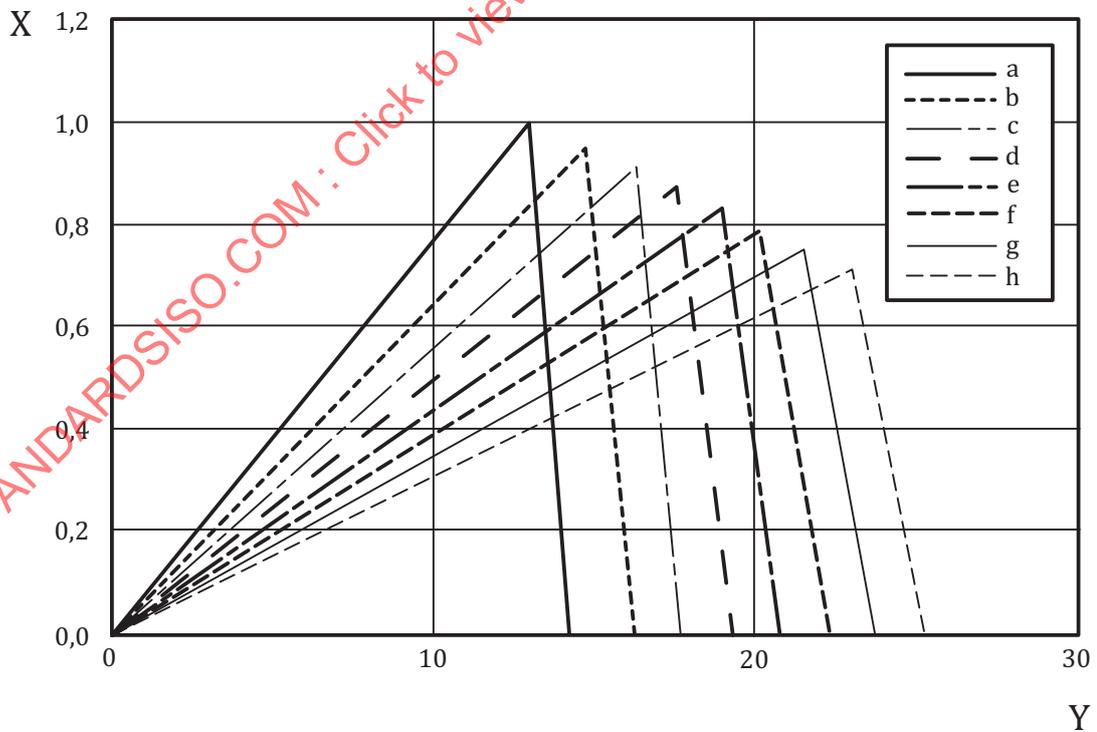

Figure 21 — Temperature dependent stress strain diagrams for clay units (type 1) with unit strength of 12 – 20 N/mm² and with a denisty range of 900 – 1 200 kg/m³
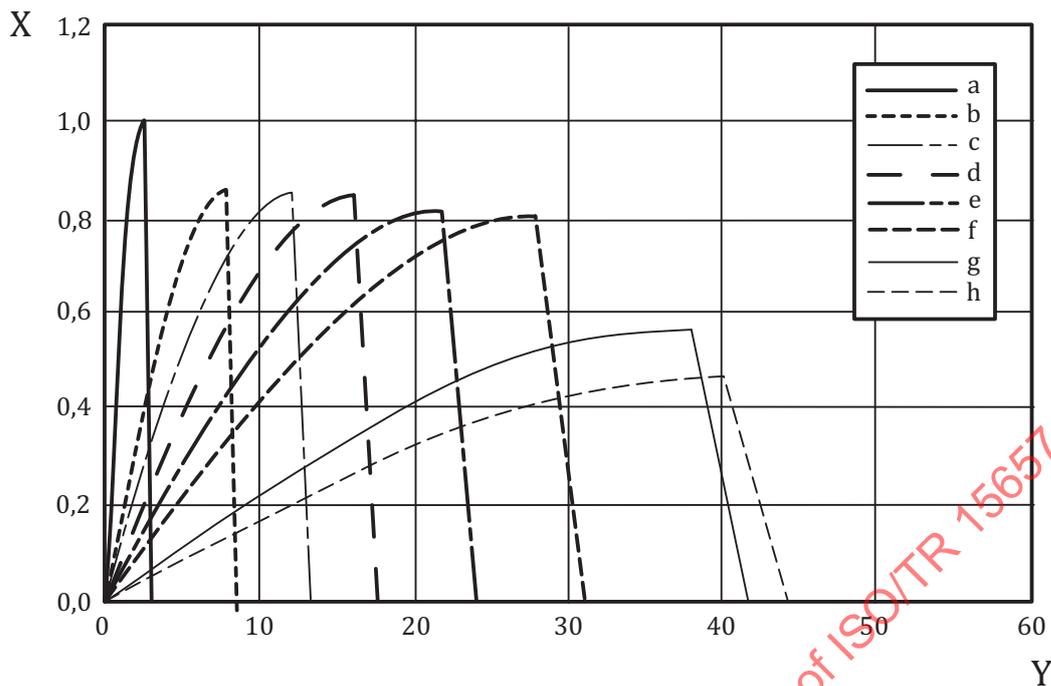
Figure 22 — Temperature dependent stress strain diagrams for calcium silicate units (solid) with unit strength of 12 – 20 N/mm² and with a denisty range of 1 600 – 2 000 kg/m³

6.1.5 Aluminium alloys

The elastic modulus of aluminium at elevated temperatures for a 2 hour exposure period is given in Table 12.

Table 12 — Elastic modulii of aluminium alloys at elevated temperatures

Temperature θ (°C)	Modulus of Elasticity $E_{al\,\theta}$ (N/mm² × 10³)
20	70.0
50	69.3
100	67.9
150	65.1
200	60.2
250	54.6
300	47.6
350	37.8
400	28.0
550	0

The strength reduction factors for aluminium alloys are given in Table 13.

Table 13 — Strength reduction values for various aluminium alloys at elevated temperatures

Alloy	Temperature	Temperature °C							
		20	100	150	200	250	300	350	550
ENAW-5052	O	1.00	1.00	0.96	0.82	0.68	0.48	0.23	0.00
ENAW-5052	H34	1.00	1.00	0.92	0.52	0.33	0.22	0.13	0.00
ENAW-5083	O	1.00	1.00	0.98	0.90	0.75	0.42	0.22	0.00
ENAW-5083	H113	1.00	1.00	0.89	0.78	0.63	0.47	0.29	0.00
ENAW-5454	O	1.00	1.00	0.96	0.88	0.50	0.32	0.21	0.00
ENAW-5454	H32	1.00	1.00	0.92	0.78	0.36	0.23	0.14	0.00
ENAW-6061	T6	1.00	1.00	0.92	0.79	0.62	0.32	0.10	0.00
ENAW-6063	T6	1.00	1.00	0.90	0.74	0.38	0.20	0.10	0.00
ENAW-6082	T6	1.00	1.00	0.79	0.65	0.38	0.20	0.11	0.00
ENAW-3003	O	1.00	1.00	0.90	0.79	0.64	0.46	0.38	0.00
ENAW-3003	H14	1.00	1.00	0.76	0.51	0.26	0.16	0.10	0.00
ENAW-5086	O	1.00	1.00	0.89	0.78	0.63	0.47	0.29	0.00
ENAW-5086	H112	1.00	1.00	0.99	0.91	0.73	0.46	0.30	0.00
ENAW-7075	T6	1.00	1.00	0.79	0.43	0.24	0.16	0.10	0.00

6.1.6 Glass

The mechanical properties of glass of all types are very variable and therefore the properties on the mechanical behaviour in Table 14 should be taken as typical rather than absolute.

Table 14 — Mechanical properties of some common glasses

Property	units	Glass Type (generic)			
		Quartz (Fused Silica)	Borosilicate	Soda Lime	Glass (Ceramic)
Density	kg/m^3	2.2	2.23	2.5	2.53
Elastic Modulus	10^4 MPa	7.2	6.3	7.3	9.1
Shear Modulus	10^4 MPa	31	-	3	-
Poisons ratio	-	0.17	0.20 (25 - 400 °C)	0.22	0.24
Max service temperature	°C	1000	500	450	600
Softening Point	°C	1683	800	726	-
Tensile Strength	Pa	70	70	-	-
Compressive Strength	MPa	1108	-	-	~2,000
Shear Strength	PA	70	-	-	-

The uncertainty concerning a characteristic value applies primarily to tensile strength, which is substantially influenced by the glassy structure. A single characteristic tensile strength value cannot be quoted. Measurement on pristine samples, for example, taken from different float lines across Europe, from different manufacturers, shows a measured range of 30 N/mm^2 to 120 N/mm^2. Strengths on freshly drawn fibres, for example, will be as high as ~5000 N/mm^2. This feature applies to all glass types, being a function of the fundamental nature of glass.

Glass ceramics fall into a different category of performance from either soda-lime or borosilicate. Although the performance under thermal stress of the ceramic type used for fire resistance is good, due to zero thermal expansion, it is brittle. Its mechanical performance, therefore, does not allow impact safety rating without laminating using an impact interlayer such as pvb. Note that "glass ceramics" refers to a group of widely differing compositions used for different applications and any quoted properties need to be specifically identified with the specific type.

6.1.7   Plastics and Resins

There is a wide range of plastics and resins that are used in load bearing construction. These may be in the form of extruded shapes such as H sections, a composite section in combination with another material e.g. steel, or as a laminate which may be used to reinforce another structural element. The majority of plastics and resins do not survive at very high temperatures, however, those that do are able to form a stable char which insulates the remainder of the section in a similar way to charred wood protects an unburnt timber.

Specific types of plastics and resins are introduced by their trade names together with some of the more common types in Table 15.

Table 15 — Mechanical properties of some common plastics

Material	Parameter						
	Density kg/m^3	Bending Strength N/mm^2	Strain @ Failure %	Compressive Strength N/mm^2	Elastic Modulus N/mm^2	Tensile Strength N/mm^2	Weakening Point (Vicat) °C
Polytetrafluorethene PTFE	2,000-2,300	18-20	300-500	10	400	17.5-26	327
Noryl	1060	95	20	115	2500	67	130
Polyfenylene-oxyde	1060	98-105	80	120	2500	75	191
Thermoplastic Polyester	1370	12.5	150	Approx 100	3500	74	Approx 150
Polyacetate	1410	110	28	90	3000	68	154
Polyamide (Nylon 6) PA	1130	27	170	90	1300	43	215-220
Acrylonitril-butadieen-styrene ABS	1070	60	3	47	2500	40	90
Polystyrene PS	1050	80	15	90	2600	42.5	70
Polymethylmethacrylate PMMA	1180	140	3.5	120	3250	75	115
Polycarbonate PC	1200	75	>110	80	2200	65	170
Polypropylene	920	45	650	46	1300	275-300	90
Soft Polyvinylchloride PVC	1200	85	370-400	75	Approx 50	16-18	50-60
Polyvinylchloride-chloride PVC-C (high temperature)	1540	Approx 100	Approx 70	70-80	800	57	105
High impact strength polyvinylchloride PVC	1380	50	60-70	110	2500	23-40	55-75
Hard-polyvinylchloride PVC	1390	80-110	20-50	80	3000	50-60	80
Perspex	1200	116	4	-	2500-3500	75	110
Nylon	1140	11	50	70	2800	86	-

The flexural strength of glass fibre reinforced polyester laminates at elelvated temperatures is given in Table 16.

Table 16 — Mechanical properties of glass re-inforced polyester laminates

Strength property, MPa	Temperature			
	20 °C	50 °C	80 °C	100 °C
Flexural strength	193	151	107	27
Flexural modulus	6896	6206	4827	2068
Tensile strength	103	82	57	20
Tensile modulus	7586	6896	5862	3448

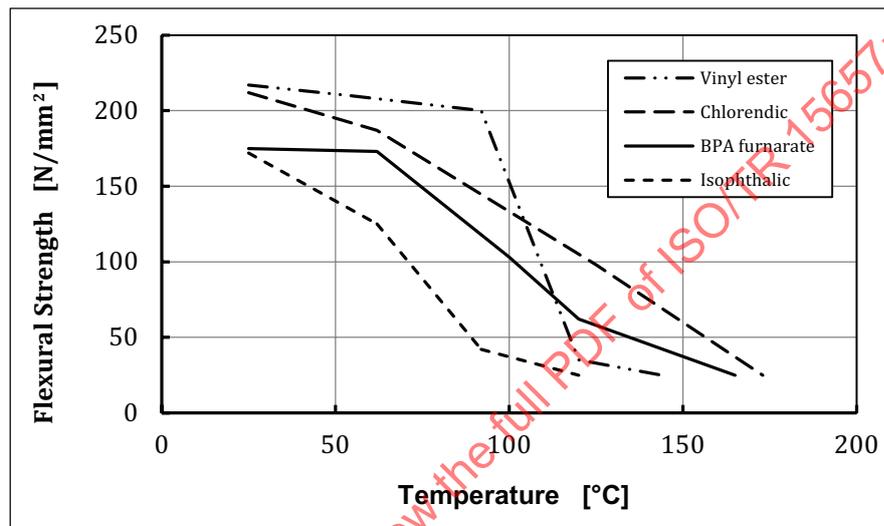The flexural strength of several composites is illustrated in Figure 23.

Figure 23 — The flexural strength of composite materials at elevated temperatures

6.2 Thermo physical properties

The following section describes the thermo-physical properties of materials that may be used to determine the mechanical behaviour of structural elements under standard furnace (nominal) heating conditions. In most cases the properties are also valid for structural elements exposed to real fires.

6.2.1 Concrete

6.2.1.1 Expansion

The thermal strain $\varepsilon_c(\theta)$ of concrete is given by:

Silaceous aggregates:

For 20 °C ≤ θ ≤ 700 °C

$$\varepsilon_c(\theta) = -1.8 \times 10^{-4} + 9 \times 10^{-6}\theta + 2.3 \times 10^{-11}\theta^3 \qquad [\text{-}]$$

(6.12)

For 700 °C < θ ≤ 1200 °C

$$\varepsilon_c(\theta) = 14 \times 10^{-3} \text{ for } 700 \text{ °C} < \theta \leq 1200 \text{ °C} \qquad [\text{-}]$$

(6.13)

Calcareous aggregates:

For 20 °C ≤ θ ≤ 805 °C

$$\varepsilon_c(\theta) = -1.1 \times 10^{-4} + 6 \times 10^{-6}\theta + 1.4 \times 10^{-11}\theta^3 \qquad [\text{-}]$$

(6.14)

For 805 °C < θ ≤ 1200 °C

$$\varepsilon_c(\theta) = 12 \times 10^{-3} \qquad [\text{-}]$$

(6.15)

These relationships are shown in Figure 24.

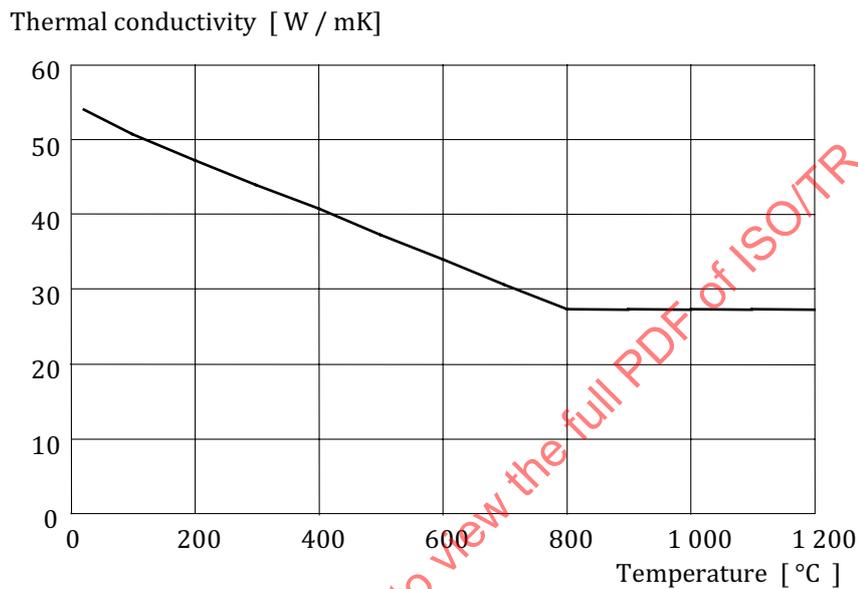Thermal conductivity [W / mK]

Figure 24 — Thermal elongation of concrete

6.2.1.2   Specific heat

The specific heat, $c_p(\theta)$, of dry concrete (moisture = 0 %) for silaceous and calcareous aggregates is given as follows:

For 20 °C ≤ θ ≤ 100 °C

$$c_p(\theta) = 900 \qquad \text{[J/kgK]}$$

(6.16)

For 100 °C < θ ≤ 200 °C

$$c_p(\theta) = 900 + (\theta - 100) \qquad \text{[J/kgK]}$$

(6.17)

For 200 °C < θ ≤ 400 °C

$$c_p(\theta) = 1000 + (\theta - 200)/2 \qquad \text{[J/kgK]}$$

(6.18)

For 400 °C < θ ≤ 1200 °C

$$c_p(\theta) = 1100 \qquad \text{[J/kgK]}$$

(6.19)

Where moisture is not considered explicitly in the calculation method specific heat of concrete can be modelled by inserting a constant value for $c_{p.peak}$ between 100 °C and 115 °C with a linear increase between 115 °C and 120 °C.

where;

For $c_{p.peak}$ = 900 [J/kgK] for moisture content of 0 % of concrete weight

For $c_{p.peak}$ = 1470 [J/kgK] for moisture content of 1.5 % of concrete weight

For $c_{p.peak}$ = 2020 [J/kgK] for moisture content of 3.0 % of concrete weight

For lightweight concrete the specific heat of 840 J/kgK can be assumed

6.2.1.3 Thermal conductivity

The thermal conductivity, λ_c, of normal weight concrete for 20 °C ≤ θ ≤ 1200 °C is given between the upper and lower bound values described by:

For the upper bound:

$$\lambda_c = 2.0 - 0.2451(\theta/100) + 0.0107(\theta/100)^2 \qquad \text{[W/mK]}$$

(6.20)

For the lower bound:

$$\lambda_c = 1.36 - 0.136(\theta/100) + 0.0057(\theta/100)^2 \qquad \text{[W/mK]}$$

(6.21)

where;

θ is the concrete temperature

6.2.1.4 Emissivity

The emissivity of conrete, ε_c, may be taken as 0.7.

6.2.2   Steel

6.2.2.1   Carbon Steel

6.2.2.1.1   Thermal elongation

The thermal elongation of steel, $\Delta l/l$ should be determined from the following:

For 20 °C ≤ θ_a ≤ 750 °C

$$\Delta l/l = 1.2 \times 10^{-5}\theta_a + 0.4 \times 10^{-8}\theta_a^2 - 2.416 \times 10^{-4} \qquad [\text{-}] \tag{6.22}$$

For 750 °C ≤ θ_a ≤ 860 °C

$$\Delta l/l = 1.1 \times 10^{-2}\theta_a \quad 750\ °C \leq \theta_a \leq 860\ °C \qquad [\text{-}] \tag{6.23}$$

For 860 °C ≤ θ_a ≤ 1200 °C

$$\Delta l/l = 2.5 \times 10^{-5}\theta_a - 6.2 \times 10^{-3} \quad 750\ °C \leq \theta_a \leq 860\ °C \qquad [\text{-}] \tag{6.24}$$

where:

l is the length at 20 °C

Δl is the temperature induced expansion

θ_a is the steel temperature [°C].

The variation of the thermal elongation with temperature is illustrated in Figure 25.

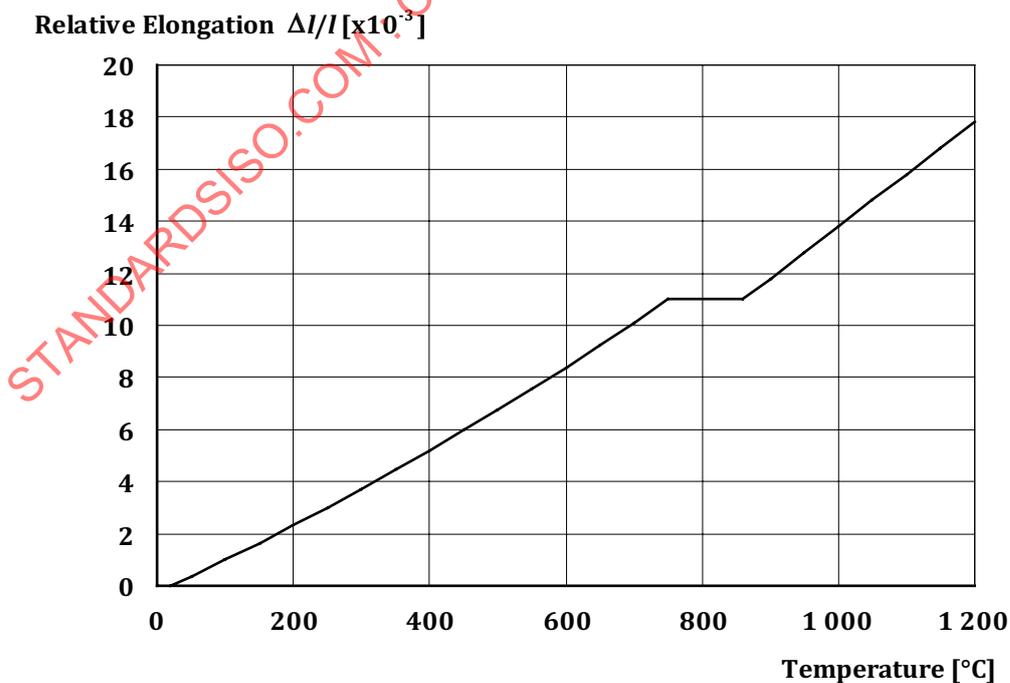**Relative Elongation $\Delta l/l$ [x10⁻³]**

Figure 25 — Thermal elongation of carbon steel as a function of the temperature

6.2.2.1.2 Specific heat

The specific heat of steel, c_a, should be determined from the following:

For 20 °C $\leq \theta_a \leq$ 600 °C

$$c_a = 425 + 7.73 \times 10^{-1} \theta_a^2 + 2.22 \times 10^{-6} \theta_a^3 \qquad [\text{J} / \text{kgK}] \tag{6.25}$$

For 600 °C $\leq \theta_a \leq$ 735 °C

$$c_a = 666 + \frac{13002}{738 - \theta_a} \qquad [\text{J} / \text{kgK}] \tag{6.26}$$

For 735 °C $\leq \theta_a \leq$ 900 °C

$$c_a = 545 + \frac{17802}{\theta_a - 731} \qquad [\text{J} / \text{kgK}] \tag{6.27}$$

For 900 °C $\leq \theta_a \leq$ 1200 °C

$$c_a = 650 \qquad [\text{J/kgK}] \tag{6.28}$$

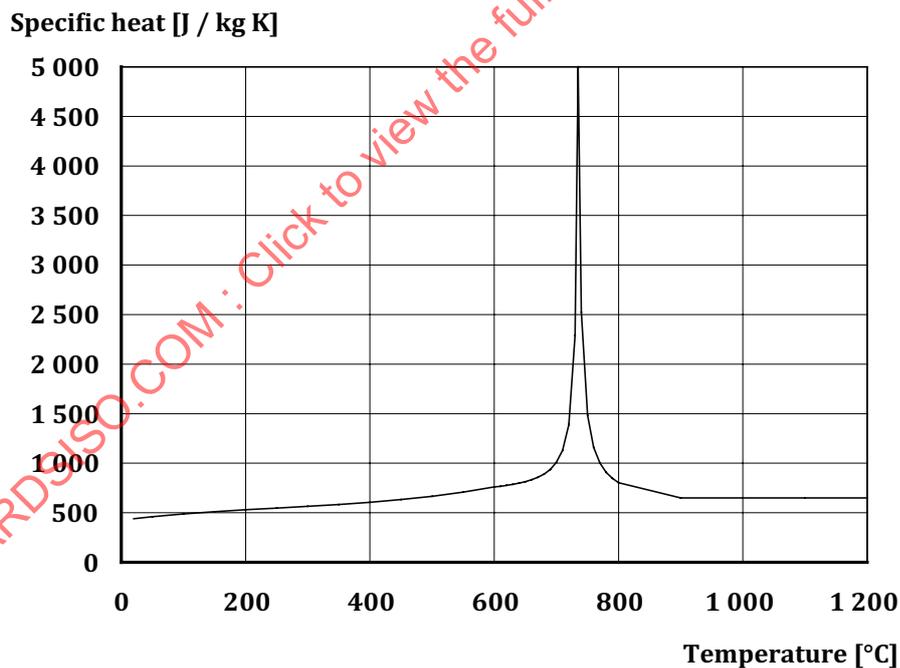The variation of the specific heat with temperature is illustrated in Figure 26.

Figure 26 — Specific heat of carbon steel as a function of the temperature

6.2.2.1.3 Thermal conductivity

The thermal conductivity of steel λ_a can be determined from the following:

For 20 °C ≤ θ_a ≤ 800 °C

$\lambda_a = 54 - 3.33 \times 10^{-2} \theta_a$ [W/mK]

(6.29)

For 800 °C ≤ θ_a ≤ 1200 °C

$\lambda_a = 27.3$ [W/mK]

(6.30)

where;

θ_a is the steel temperature [°C]

The variation of the thermal conductivity with temperature is illustrated in Figure 27.

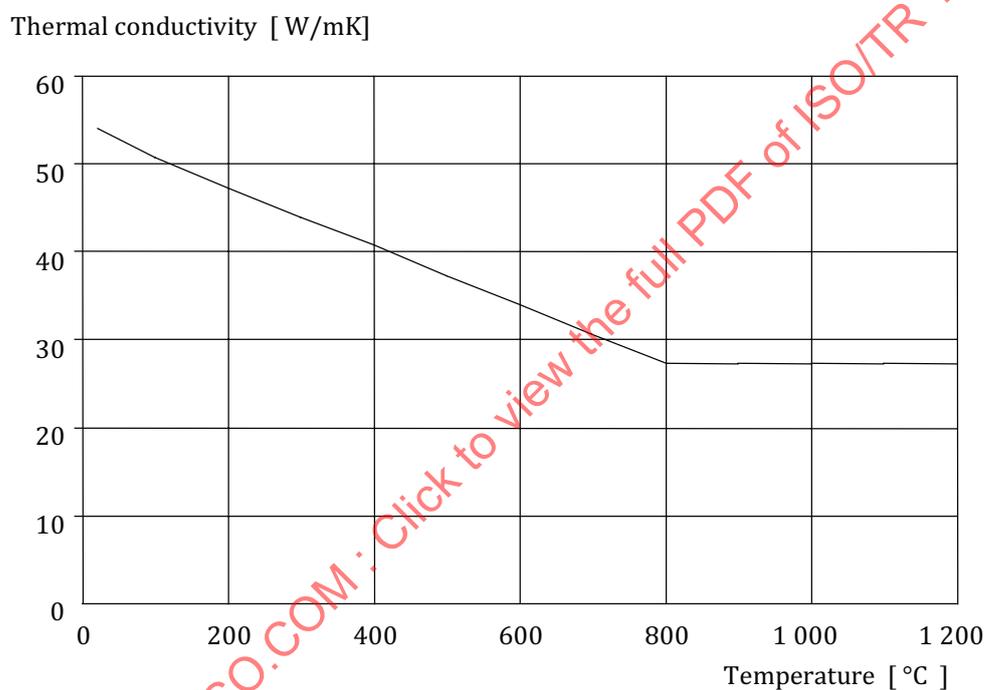Thermal conductivity [W/mK]

Figure 27 — Thermal conductivity of carbon steel as a function of temperature

6.2.2.2   Stainless steel

6.2.2.2.1   Thermal elongation

The thermal elongation of austenitic stainless steel, $\Delta l / l$, may be determined from the following:

$$\Delta l / l = \left(16 + 4.79 \times 10^{-2} \theta_a - 1.243 \times 10^{-8} \theta_a^2\right) \times \left(\theta_a - 20\right) \times 10^{-6} \qquad [-] \qquad (6.31)$$

where;

l is the length at 20 °C

Δl is the temperature induced expansion

θ_a is the steel temperature [°C]

6.2.2.2.2   Specific heat

The specific heat of stainless steel, c_a, may be determined from the following:

$$c_a = 450 + 0.280 \times \theta_a - 2.91 \times 10^{-4} \theta_a^2 + 1.34 \times 10^{-7} \theta_a^2 \qquad [J / Kgk] \qquad (6.32)$$

where;

θ_a is the steel temperature [°C]

6.2.2.3   Thermal conductivity

The thermal conductivity of stainless steel λ_a can be determined from the following:

$$\lambda_a = 14.6 + 1.27 \times 10^{-2} \theta_a \qquad [W/mK]$$

$$(6.33)$$

where;

θ_a is the steel temperature [°C]

6.2.3   Timber

For standard exposure conditions the following thermal properties apply:

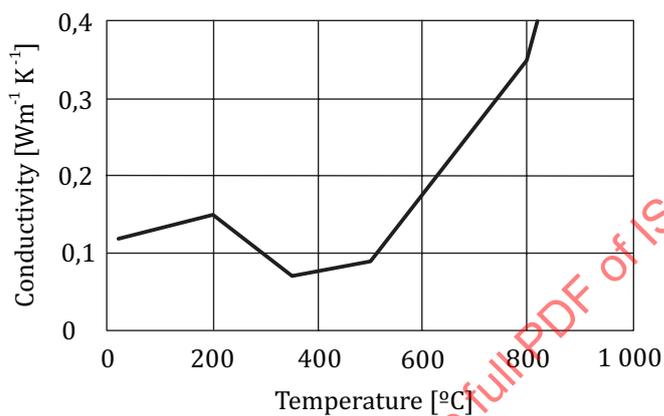### 6.2.3.1   Thermal conductivity

The thermal conductivity values of the char layer are apparent rather than measured values of charcoal in order to take into account increased heat transfer due to shrinkage cracks above ~500 °C and the consumption of the char layer at ~1000 °C

Depending upon the model used for calculation modification of the thermal properties may be necessary.

The variation in thermal conductivity of timber with temperature is given in Table 17 and illustrated in Figure 28.

Table 17 — Temperature dependence of the thermal conductivity of timber

Temperature	Thermal conductivity
°C	$Wm^{-1}K^{-1}$
20	0,12
200	0,15
350	0,07
500	0,09
800	0,35
1200	1,50

Figure 28 — Temperature dependence of the thermal conductivity of timber

6.2.3.2 Specific heat capacity an density

The specific heat capacity and ratio of density to dry density of softwood at elevated temperatures for service class 1 as defined in Eurocode 5 is given in Table 18.

Table 18 — Temperature dependence of specific heat capacity and density ratio of softwood

Temperature °C	Specific heat capacity kJ kg-1 K-1	Density ratio[a]
20	1,53	1 + w
99	1,77	1 + w
99	13,60	1 + w
120	13,50	1,00
120	2,12	1,00
200	2,00	1,00
250	1,62	0,93
300	0,71	0,76
350	0,85	0,52
400	1,00	0,38
600	1,40	0,28
800	1,65	0,26
1200	1,65	0
[a] w is the moisture content		

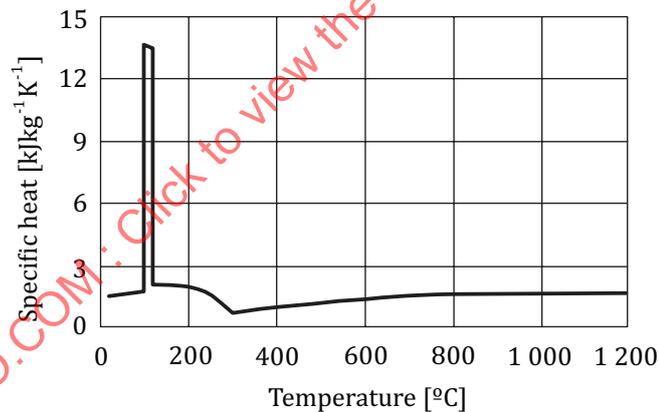The variation in specific heat of wood and charcoal at elevated temperatures is shown in Figure 29.

Figure 29 — Temperature dependence of specific heat of wood and charcoal at elevated temperatures

The temperature density ratio of softwood with an initial moisture content of 12 % can be described as shown in Figure 30.
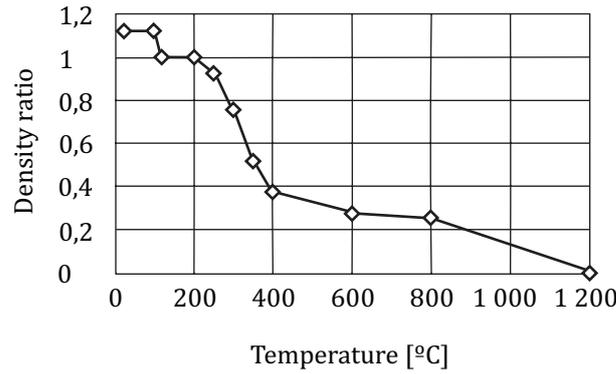
Figure 30 — Temperature density ratio for softwood with an initial 12 % moisture content

6.2.3.3 Charring rate of timber

The charring depth is the distance between the outer surface of the original member and the position of the char-line and can be calculated from the time of fire exposure and the relevant charring rate.

The calculation of cross-sectional properties should be based on the actual charring depth including corner roundings. Alternatively a notional cross-section without corner roundings may be calculated based on the notional charring rate. The position of the char-line should be taken as the 300-degree isotherm.

The charring rate for one-dimensional charring under standard furnace conditions can be taken as constant with time and calculated from:

$$d_{char,0} - \beta_0 t \qquad \text{[mm]} \tag{6.34}$$

where;

$d_{char,0}$	is the design charring depth for one dimensional modelling	[mm]
β_0	is the notional one dimensional charring rate under standard exposure	[mm/min]
t	is the time of fire exposure	[min]

The notional charring rate which includes for the effect of corner roundings and fissures should be taken as constant with time and can be calculated from:

$$d_{char,n} - \beta_n t \qquad \text{[mm]} \tag{6.35}$$

where;

$d_{char,n}$	is the design charring depth, which incorporates the effect of corner roundings	[mm]
β_n	is the one dimensional charring rate under standard exposure	[mm/min]
t	is the time of fire exposure	[min]

For surfaces of timber, unprotected throughout the time of fire exposure, design charring rates, $d_{char,0}$ and $d_{char,n}$ are given in Table 19.